DOI: 10.1002/ejic.200600016

Octahedral Ru^{II} Complexes with [PNO] Hydrazonic Ligands: Synthesis, Structure, Reactivity and Catalytic Activity in the Addition of Benzoic Acid to Alkynes

Paolo Pelagatti,*[a] Alessia Bacchi,[a] Marcella Balordi,[a] Sandra Bolaño,[b][‡] Francesca Calbiani,[a] Lisa Elviri,[a] Luca Gonsalvi,*[b] Corrado Pelizzi,[a] Maurizio Peruzzini,[b] and Dominga Rogolino[a]

Keywords: Tridentate ligands / Ruthenium / Homogeneous catalysis / Enol esters / Mass spectrometry

A series of Ru^{II} complexes containing [(H)PNO] hydrazonic ligands were synthesised using different ruthenium sources such as $[Ru(PPh_3)_3Cl_2]$, $[Ru(dmso)_4Cl_2]$ and $[Ru(p\text{-cymene})Cl_2]_2$. The complexes were characterised by ^1H NMR, $^{31}P\{^1H\}$ NMR, IR, FAB-MS, microanalysis and in some cases by X-ray diffraction analysis on a single crystal. The ligands show a great variety of different coordinating behaviours such as κ^3-(H)PNO, κ^2-(H)PN, κ^1-(H)P and κ^3-PNO, depending on the ruthenium precursor and on the synthetic experimental conditions. The complexes *trans*-$[Ru(\kappa^3\text{-(H)PNO})(PPh_3)Cl_2]$ reacted with dmso to give the bis-chelate complex $[Ru(\kappa^3\text{-PNO})_2]$, $[Ru(dmso)_4]Cl_2$, $OPPh_3$, HCl and Me_2S, through an oxygen-transfer reaction from dmso to PPh_3. A catalytic version of this reaction was also developed. The complexes obtained from $[Ru(PPh_3)_3Cl_2]$ were tested as homogeneous pre-catalysts for the coupling between benzoic acid and terminal alkynes to give the corresponding enol esters. High stereo- and regio-selectivity, up to 100 % (determined by ^1H NMR), in favour of the (*Z*)-*anti*-Markovnikov products (*Z*)-alk-1-en-1-yl benzoate was observed. An ESI-MS monitoring of the catalytic couplings revealed that the enol ester formation occurs through an intermolecular attack of an external carboxylate anion onto a vinylidene–Ru intermediate of the type $[Ru(PNO)(PPh_3)(C{=}CH{-}C_4H_9)Cl]$.

Introduction

The use of potentially tridentate [PNO] ligands in the synthesis of transition-metal complexes is scarcely described in the literature.[1] However, Ru^{II} complexes with [PNO] ligands have been shown to be active catalysts in the transfer hydrogenation of ketones,[2] and some of us have reported that [Pd(PNO)(OAc)] and [Pd(PNO)Cl] complexes [PNO = acylhydrazones] promote the catalytic homogeneous hydrogenation of alkenes[3] and the semi-hydrogenation of terminal alkynes,[4] respectively. The use of [PNO] ligands for the preparation of homogeneous catalysts containing *soft* transition metals, is based on two assumptions: *i*) that the chelating PN unit stabilizes the metal fragment under the catalytic conditions and *ii*) that the labile M–O bond makes reactive the metal complex exerting, at the same time, a control upon the accessibility at the metal for an incoming substrate. This last feature can be determinant for the selectivity of the catalytic process. When the [PNO] ligand is protic, as in the case of the acyl hydrazones, a further control on the hemilability of the ligand, from a κ^3-(H)PNO coordination to a κ^2-(H)PN one, as well as on the nucleophilicity of the metal, can be exerted as a function of the anionic or neutral character of the ligand.[5]

As our ongoing research on the use of protic [PNO] acyl hydrazones as ligands in the synthesis of transition-metal-containing complexes,[5] we have undertaken a study on the coordinating behaviour of 2-(diphenylphosphanyl)benzaldehyde benzoylhydrazone (Hbidf) and 2-(diphenylphosphanyl)benzaldehyde acetylhydrazone (Haidf) (Scheme 1), towards Ru^{II}.

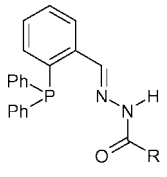

R = Ph **Hbidf**
Me **Haidf**

Scheme 1.

[a] Dipartimento di Chimica Generale ed Inorganica, Chimica Analitica, Chimica Fisica, Università degli Studi di Parma, Parco Area delle Scienze 17/A, 43100 Parma, Italy
E-mail: paolo.pelagatti@unipr.it
[b] Istituto di Chimica dei Composti Organometallici, Consiglio Nazionale delle Ricerche (ICCOM-CNR), via Madonna del Piano 10, 50019 Sesto Fiorentino, Firenze, Italy
E-mail: l.gonsalvi@iccom.cnr.it
[‡] Current address: Universidad de Vigo, Facultad de Ciencias (Químicas), Campus Universitario, 36310 Lagoas Marcosende, Vigo, Spain
Supporting information for this article is available on the WWW under http://www.eurjic.org or from the author.

The two ligands have been reacted with $[Ru(PPh_3)_3Cl_2]$ under different reaction conditions, in order to isolate neutral or ionic complexes containing the ligands in either protonated or deprotonated form. All the complexes have been fully characterised by a number of analytical and spectroscopic techniques and, in several cases, by X-ray diffraction analysis on a single crystal. In order to elucidate the reactivity shown by the complexes of the type $[Ru(\kappa^3\text{-}HPNO)(PPh_3)Cl_2]$ with dmso, the syntheses and the characterisations of various Ru complexes obtained by reactions of Hbidf with $[Ru(dmso)_4Cl_2]$ and $[Ru(p\text{-cymene})Cl_2]_2$ are also reported.

Ruthenium is certainly one of the mostly used transition metals in homogeneous catalysis.[6] The Ru-promoted coupling between benzoic acid and terminal alkynes (Scheme 2) is an elegant way to produce vinyl esters, which find industrial applications as polymerising substrates[7] and acylating reagents for the synthesis of amides[8] and halogenated ketones;[9] other applications include cyclopropanation,[10] 1,3-dipolar cycloaddition,[11] asymmetric hydrogenation[12] and hydroformylation reactions.[13]

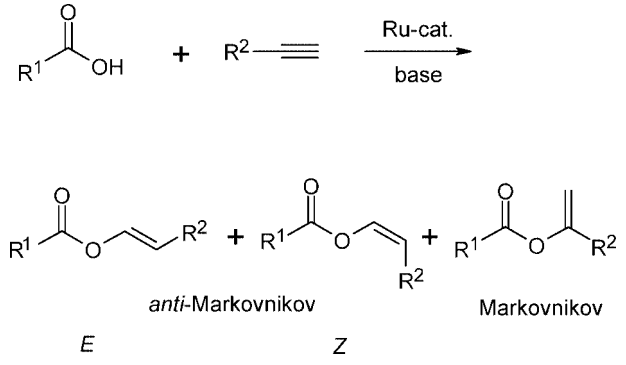

Scheme 2.

The first report describing this reaction dates back to 1983[14] and deals with the use of $Ru_3(CO)_{12}$ in the coupling of aliphatic and aromatic carboxylic acids to di- and monosubstituted acetylenes. Later on, the process has been developed by Mitsudo,[15] Dixneuf[16] and Verpoort,[17] although other groups have been and are still involved in the field.[18] From the literature it can be inferred that the combination of monodentate phosphanes with different Ru sources generally yields to the Markovnikov product,[15,16a,16b,19] although in some cases the selectivity can be switched to the *anti*-Markovnikov product by replacing inorganic bases with organic (coordinating) ones, such as pyridine derivatives.[18] The same trend has been described by Dixneuf replacing mono- with chelating phosphanes[16d] and by Verpoort adding phosphanes to N-heterocyclic carbene complexes.[17d] With this in our mind, we have argued that the high chelation degree of the acyl hydrazones could induce a good selectivity towards the *anti*-Markovnikov products, thus leading to the formation of the less commonly obtained isomer. In order to test this hypothesis and because of the lack of data concerning the use of pre-catalysts containing tridentate ligands for this particular coupling reaction, we have decided to test the complexes deriving from the combinations of Hbidf and Haidf with $[Ru(PPh_3)_3Cl_2]$ as pre-catalysts in the addition of benzoic acid to terminal alkynes. Aiming at detecting the organometallic intermediates involved in the catalytic cycle, an ESI-MS study has been performed. ESI-MS technique allows for the detection of species at low concentration in solution and this makes it attractive to define the mechanism of metal-promoted catalytic transformations. It has been successfully employed in different reactions, such as the reduction of ketones,[20] epoxidations,[21] olefins polymerisation[22] and C–H bonds activation.[23] To the best of our knowledge, this is the first report dealing with the application of such a technique for the study of the addition of carboxylic acids to alkynes.

Results and Discussion

Selected spectroscopic data ($^{31}P\{^1H\}$NMR, ^1H NMR and FT-IR) of the complexes reported in this work are collected in Table 1.

Ru Complexes Obtained from $[Ru(PPh_3)_3Cl_2]$

The free ligands Hbidf and Haidf react with a stoichiometric amount of $[Ru(PPh_3)_3Cl_2]$ in dichloromethane at room temperature, leading to the neutral dichloride complexes *trans*-$[Ru(\kappa^3\text{-}(H)PNO)(PPh_3)Cl_2]$, which were isolated as purple solids in good yields (**1** and **2** in Scheme 3, respectively).

The neutral hydrazones coordinate in a tridentate fashion by means of the P, N_{imine} and O donors. The neutral behaviour of the ligands is indicated by the IR stretching bands of the N–H bonds (3148 and 3145 cm^{-1} for **1** and **2**, respectively), while the involvement of the carbonyl group in the coordination is pointed out by the shift to lower wavenumbers of the C=O stretching band (1629 cm^{-1} for both complexes) with respect to the free ligands (1652 and 1678 cm^{-1} for Hbidf and Haidf, respectively). The octahedral coordinations are completed by a PPh_3 molecule and by two chloride ligands. The FAB-MS spectra and the elemental analyses confirm the proposed stoichiometries. The complexes **1** and **2** are poorly soluble in chloroform, dichloromethane, THF, toluene, acetonitrile and methanol, while they readily dissolve in strongly coordinating solvents, like dmso and dmf. Based on the reactivity of **1** observed in warm acetonitrile (vide infra), we suppose that the solution of **1** and **2** in dmso or dmf occurs by breaking of a Ru–Cl bond and formation of the cationic complexes $[Ru(\kappa^3\text{-}(H)PNO)(PPh_3)(S)Cl]Cl$ (**1a** and **2a**, S = dmso or dmf). The ^1H NMR spectra of the freshly prepared samples recorded in $[D_6]$dmso show singlets belonging to the hydrazonic protons at δ = 14.11 and 13.65 ppm for **1a** and **2a**, respectively, while the HC=N protons give rise to doublets at δ = 9.14 ppm and 8.69 ppm, respectively. The somewhat high $^4J_{PH}$ values of 7.5 and 7.7 Hz for **1a** and **2a**, respectively, corresponding to the couplings between the iminic protons

Table 1. Selected spectroscopic signals of the Ru complexes.

Complex	$^{31}P\{^1H\}$ NMR[a]			^1H NMR [δ][a]		IR [cm^{-1}][b]	
	PPh_2	PPh_3	$^2J_{PP}$ [Hz]	N–H	HC=N [$^4J_{PH}$]	ν(NH)	ν(C=O)
1						3148 (w)	1629 (s)
1a[c]	63	39.1	32	14.11	9.14 (7.5)		
1b[c]	49	32	26.5		9.14 (8.2)		
1c	54	34	30				
2						3145 (w)	1629 (s)
2a[c]	65.3	40.8	31	13.65	8.69 (7.7)		
2b[c]	53.1	33.9	28				
3	56.1	38.6	24	–	9.06 (8.1)	absent	absent
4	54.9	37.4	24	–	8.85 (br)	absent	absent
5	59.3	40	29	n.d.	9.24 (8.1)	3168 (w)	1624 (s)
6	56.4	35.6	27	14.31	8.88 (br)	3180 (w)	1625 (s)
7	57.9	38.3	24	n.d.	9.12 (7.2)	3259 (w)	1612 (m)
8	55.5	37.7	28	10.53	7.69 (br)	3267 (w)	1630 (m)
9	54.8	38.3	22	–	9.04 (8.1)	absent	absent
10	50.4	30.8	br. s	–	8.87 (br)	absent	absent
12	57.7 (s)			–	9.18 (s)	absent	absent
13	45.5 (s)			11.24	9.15 (s)	3294 (w)	1674 (s)
14	61 (s)			10.34	8.53 (s)	3156 (w)	1594 (s)
15	29.6			10.31	9.08 (s)	3311 (w)	1696 (s)

[a] CD_2Cl_2. [b] KBr disks. [c] $[D_6]$dmso.

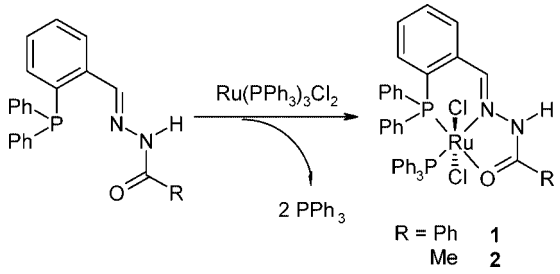

Scheme 3.

and the P atoms of the PPh_3 (as established by heteronuclear ^1H-^{31}P correlation), are indicative of a PPh_3 molecule *trans* to the HC=N function.[24] The chloride ligand and dmso occupy the apices of the octahedron. The stereoselectivity of the reaction is indicated by $^{31}P\{^1H\}$-NMR spectroscopy by two doublets centred at 63 and 39.1 ppm for **1a** and 65.3 and 40.8 ppm for **2a**. The more shielded signals are generated by the PPh_3 ligands, while the signals at lower fields are generated by the hydrazonic phosphorus nuclei.[24] The small $^2J_{PP}$ values of 32 and 31 Hz for **1a** and **2a**, respectively, are in agreement with a *cis* arrangement of the two P atoms. The isolation of the cationic complexes **1a** and **2a** is not possible because of their reactivity with dmso, as shown by NMR spectroscopy. In fact, on keeping the NMR sample of **1a** at room temperature overnight, two additional $^{31}P\{^1H\}$-NMR doublets appear, centred at δ = 49 and 32 ppm ($^2J_{PP}$ = 26.5 Hz). Moreover, two small singlets at δ = 53 and 27 ppm are also visible (see Supporting Information; see also the footnote on the first page of this article). When the tube is warmed at 50 °C for 6 hours, the new signals grow at the expenses of those belonging to the starting complex, and an additional pair of doublets centred at δ = 54 and 34 ppm ($^2J_{PP}$ = 30 Hz) appears. After 16 hours at 50 °C, the main signals are still those of **1a**, but the singlets at δ = 53 and 27 ppm have grown considerably while the other two pairs of doublets have diminished. Finally, after 48 hours the spectrum shows only the singlets at δ = 55 and 29 ppm. The low $^2J_{PP}$ values of the two transient pairs of doublets indicate the formation of two labile Ru complexes containing two mutually *cis* phosphanes, while the final singlets are ascribable to $OPPh_3$ (singlet at δ = 29 ppm[25]) and to the bis-chelate complex $[Ru(bidf)_2]$ (**12**, singlet at δ = 55 ppm). The presence of **12** is confirmed by ESI-MS analysis of the warm dmso solution by a cluster at m/z = 917. Complex **12** can be prepared by reaction between $[Ru(PPh_3)_3Cl_2]$ or $[Ru(dmso)_4Cl_2]$ with a twofold excess of Hbidf (vide infra) in the presence of a base. Its $^{31}P\{^1H\}$-NMR spectrum shows a singlet at δ = 57.7 ppm, which is in good agreement with the value observed for the in situ formed complex. On the basis of the aforementioned observations we propose that the **1** → **12** transformation occurs in agreement with Scheme 4.

Although the detection of $(CH_3)_2S$ is made difficult by its volatility, a singlet at δ = 2.08 ppm is observed during ^1H NMR monitoring of the reaction. The same technique has allowed the detection of $[Ru(dmso)_4Cl_2]$: by repeating the **1** → **12** transformation in dmso, after the complete removal of the solvent, the ^1H NMR spectrum of the solid residue recorded in $CDCl_3$ shows, apart from the signals ascribable to **12**, singlets in the region 3.47–2.25 ppm, indicative of the presence of a mixture of *trans*- and *cis*-$[Ru(dmso)_4Cl_2]$.[26] The **1** → **12** transformation must necessarily occur through the transfer of a PNO ligand from a Ru nucleus to another one. Thus, the changes observed in the $^{31}P\{^1H\}$-NMR spectrum of **1a** in dmso may be tentatively explained as follows (Scheme 4): dmso reacts with **1a** causing the displacement of the C=O group of the ligand giving rise to $[Ru(\kappa^2\text{-}(H)PN)(PPh_3)(dmso)_2Cl]Cl$ (**1b**). Complex **1b** gives rise to the pair of doublets at δ = 49 and 32 ppm, where the more shielded signal is due to PPh_3 while the other is due to the PPh_2 moiety. The chemical shift of 49 ppm is similar to that found for **13** (δ =45.5 ppm, vide

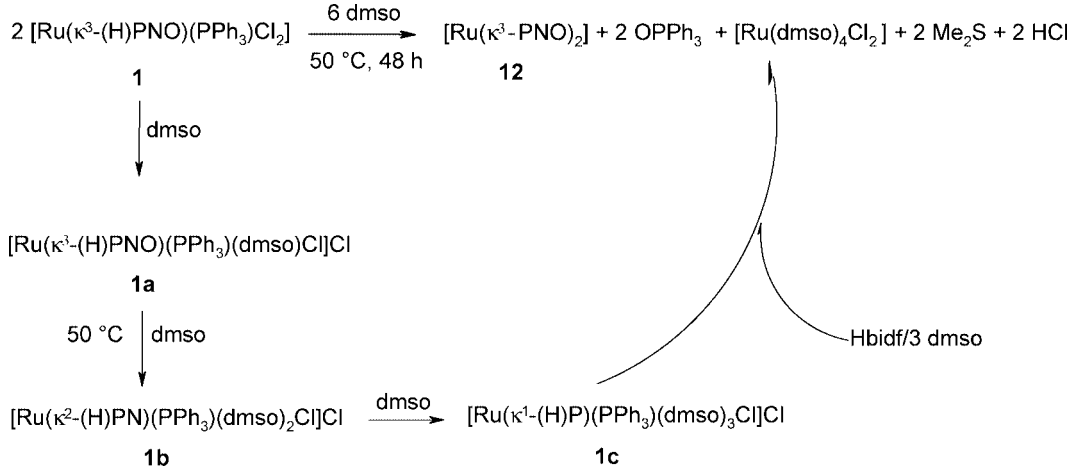

Scheme 4.

infra), where Hbidf coordinates in a (H)PN bidentate fashion. The simple isomerisation of **1b** due, for example, to the shift of PPh_3 from the plane to an apex of the octahedron is ruled out by the ^1H NMR monitoring of the process: the HC=N function of **1b** gives rise to a doublet centred at δ = 9.14 ppm with a $^4J_{PH}$ of 8.02 Hz, indicative of a PPh_3 *trans* to the imine function. The reaction continues with the decoordination of the imine nitrogen from ruthenium which is replaced by an additional molecule of dmso (probably favoured by the *trans* effect of PPh_3), with formation of complex **1c** in which the neutral ligand coordinates in an unidentate fashion through the P atom, giving rise to the pair of doublets at δ = 54 and 34 ppm. Although one would expect a decrease of the chemical shift on passing from **1b** to **1c** due to the loss of the chelation ring,[27] a chemical shift around 50 ppm is not unusual for Ru complexes containing coordinated monophosphanes and dmso.[28] Moreover, the ability of Hbidf to coordinate Ru in a P-monodentate mode is confirmed by the complex [(η^6-*p*-cymene)-Ru(κ^1-(H)P)Cl_2]·3/2 $CHCl_3$ (**15**, vide infra) obtained by the reaction of Hbidf with [Ru(*p*-cymene)Cl_2]$_2$. Finally, **1c** further transforms, through a not yet defined pathway, into [Ru(dmso)$_4Cl_2$], $OPPh_3$, $(CH_3)_2S$, HCl and **12**. PPh_3 oxidation then occurs through the dmso reduction to dimethyl sulfide. The metal ion-mediated deoxygenation of coordinated sulfoxides has been observed with different metals.[29] The most intensively studied systems are based on oxorhenium[30] and oxomolybdenum compounds,[25,31] the last also being good models of the enzymes belonging to the dmso reductase class.[32] To the best of our knowledge, the only article dealing with the deoxygenation of dmso promoted by ruthenium has been reported by James, describing the reaction of $RuCl_3$·3 H_2O with dmso at high temperatures in the presence of HCl or HBr;[33] in those cases however, although dimethyl sulfide complexes were isolated, the nature of the reductants remained unknown. Interestingly, the oxygen transfer from dmso to PPh_3 promoted by **1** can be made catalytic by dissolving the complex in dmso and heating the solution at 100 °C in the presence of a 100-fold excess of PPh_3; the reaction is complete within 20 hours as indicated by $^{31}P\{^1H\}$-NMR spectroscopy (disappearance of the PPh_3 signal at –7.5 ppm in favour of the $OPPh_3$ signal at δ = 26.8 ppm). A similar behaviour is conjecturable also for complex **2**, although its reactivity in dmso has not been investigated in details. It is worth noting that this step-by-step ligand decoordination probably corresponds to the reversed way the ligand approaches the metal, a process not always easy to envision with polydentate ligands. The key-role played by dmso in the **1** → **12** transformation is evidenced by the different reactivity shown by **1** in acetonitrile at 50 °C. After 4 hours an almost clear solution has been obtained and the work-up has led to the cationic monochelate complex [Ru(κ^3-(H)PNO)(PPh_3)(CH_3CN)Cl]Cl (**11**). The neutral character of the ligand is clearly pointed out by the IR and ^1H NMR spectra with a weak band at 3173 cm^{-1} and a singlet at δ = 10.48 ppm, respectively. The coordinated acetonitrile gives rise to a weak IR band at 2273 cm^{-1} and a singlet at δ = 1.31 ppm in the ^1H NMR spectrum. Complex **11** decomposes within 24 hours in solution and within 24–48 hours in the solid state, without evidencing the formation of **12**.

Treatment of a toluene suspension of **1** or **2** with an excess of triethylamine in the presence of acetonitrile, leads to the isolation of the neutral monochloride complexes [Ru(κ^3-PNO)(PPh_3)(CH_3CN)Cl] (**3** and **4** in Scheme 5) as yellow solids in good yields. The reactions occur with the substitution of a chloride ligand (precipitated as Et_3NHCl) with an acetonitrile molecule.

The anionic character of the ligand is indicated by the disappearance of the spectroscopic signals of the N–H and C=O bonds.[5] The coupling constants between the P nuclei are again small (24 Hz) to indicate a *cis* arrangement of the PPh_3 and PPh_2 moieties, while the iminic protons give rise to doublets with appreciable $^4J_{PH}$ values indicative of a HC=N group *trans* to a PPh_3[24] (Table 1). The coordinated acetonitrile gives a singlet at δ = 1.21 ppm in both complexes. The FAB-MS spectrum of **3** shows a cluster centred at *m*/*z* = 806 corresponding to the [Ru(κ^3-PNO)(PPh_3)Cl]$^+$ fragment, while in the FAB-MS spectrum of **4** the molecular peak is visible at *m*/*z* = 786. By slow evaporation of a

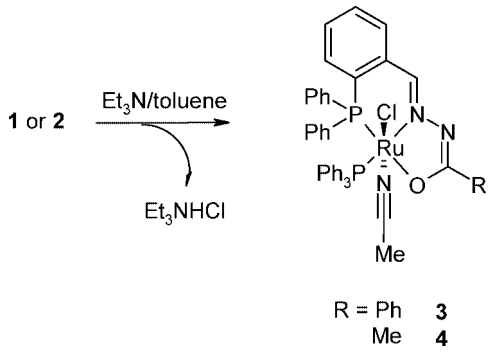

Scheme 5.

dichloromethane/acetonitrile mixture of **4**, crystals suitable for X-ray diffraction have been collected, and the structure of the complex has been unequivocally confirmed. Compound **4** crystallises with the inclusion of two water molecules in the asymmetric unit, which take part in the packing interactions. In **4** the Ru atom is hexacoordinate by the tridentate deprotonated PNO (aidf$^-$) ligand, one triphenylphosphane, *trans* to the N donor, one chloride and one acetonitrile molecule, *trans* each other, in an irregular octahedral geometry. The molecular structure is shown in Figure 1, along with the labelling scheme, while the most relevant geometric features are collected in Table 2.

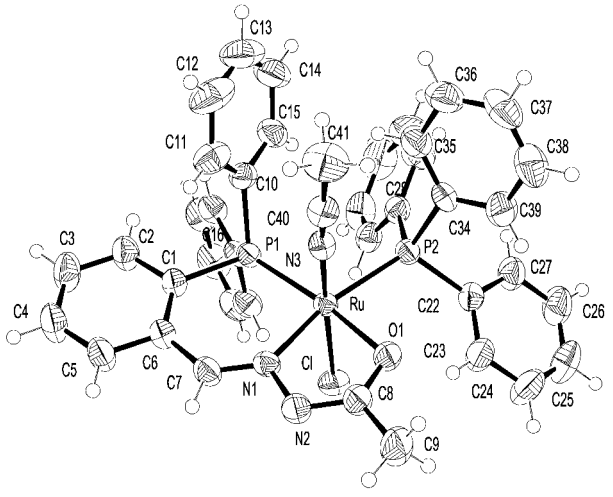

Figure 1. Perspective view and labelling scheme of compound **4**. Rings C16–C21 and C28–C33 are labelled only on the *ipso* carbon for clarity. Thermal ellipsoids at the 50% level.

The tridentate PNO coordination of aidf$^-$ gives rise to two chelation rings, which are both planar within 0.06 Å. The planarity of the six-membered chelation ring containing P1 contrasts with the behaviour generally observed in the family of the similar Pd(aidf) and Pd(bidf) complexes,[3,5c] where the chelation ring is puckered and the phosphorus donor is remarkably out of the average ring plane (values ranging between 0.38 and 0.52 Å). In fact, in the Pd series the Pd–P distances range from 2.184 to 2.212 Å, while in **4** the Ru–P bond is significantly longer [2.2951(3) Å], and can accommodate for ring planarity. By contrast, even if the Ru–O bond [2.1177(5) Å] is longer than the Pd–O bond (2.065 Å) in the [Pd(aidf)(OAc)] analogue,[3] the ligand bond lengths along the five-membered chelation ring are very close to those observed in the palladium complex, from which they do not deviate by more than 0.013 Å. The molecular association in the crystal is based on dimeric aggregates composed by two complexes related by a crystallographic twofold axis, linked by two water molecules which act as hydrogen-bond donors towards chloride and nitrogen as shown in Figure 2 [O2···N2: 2.883(2) Å, O2–H···N2: 149.7(6)°; O2···Cl(i): 2.232(1) Å, O2–H···Cl(i): 152.6(4)°, i: $y, x, 1-z$]. This pattern is conserved in the related structure of **6**.

The dichloride complexes **1** and **2** suspended in a dichloromethane/acetonitrile mixture react with an excess of KPF_6 or $NaBPh_4$ leading to the cationic monochloride complexes [Ru(κ^3-(H)PNO)(PPh_3)(CH_3CN)Cl][X] [HPNO = Hbidf, X = PF_6 (**5**), X = BPh_4 (**7**); HPNO = Haidf, X = PF_6 (**6**), X = BPh_4 (**8**)] and precipitation of KCl or NaCl, respectively (Scheme 6).

As can be inferred from Table 1, the spectroscopic characterisation indicates that the ligands have not varied their coordinating behaviour with respect to the dichloride precursors, and that the PPh_3 ligands are still *trans* to the HC=N moieties [the $^{31}P\{^1H\}$-NMR signals range from 55.5 to 59.3 ppm for the PPh_2 moiety, and from 35.6 to 40.0 ppm for the PPh_3 ligand, with $^2J_{PP}$ values ranging from 24.6 to 29 Hz; the $^4J_{PH}$ values range from 7.2 to 8.1 Hz]. The apices of the octahedron are occupied by the residual chloride and by an acetonitrile molecule, whose presence is confirmed by IR (stretching band in the region 2265–2281 cm^{-1}) and ^1H NMR spectroscopy (singlets ranging from 0.43 to 1.70 ppm). The [PF_6]$^-$ anions originate, in the $^{31}P\{^1H\}$-NMR spectra, multiplets centred at –141.1 and –145.5 ppm, for **5** and **6**, respectively, while in the IR spectra they give rise to an intense band at 845 cm^{-1}. The presence of the [BPh_4]$^-$ anion in **7** and **8** is pointed out by IR bands at about 850 cm^{-1}. The structure of **6** has been unequivocally established by X-ray diffraction analysis conducted on a single crystal grown in a CH_2Cl_2/*n*-pentane mixture. In compound **6**, the [Ru(Haidf)]$^+$ cation (Figure 3) is arranged identically to the related deprotonated neutral complex **4**.

The comparison between the two molecules (Figure 4, Table 2) may help to investigate the effect of protonation on [Ru(aidf)(PPh_3)(CH_3CN)Cl]. The protonation of the hydrazonic nitrogen N2 seems to localize a larger double-bond character on the carbonylic bond, which shortens by 0.055 Å, while at the same time the adjacent C(O)–N bond elongates by 0.016 Å. Moreover, in the cationic complex **6** the Ru–O bond is longer than in **4** by 0.028 Å, while Ru–P bond is slightly shorter (0.017 Å). The shortening of the Ru–P bond is accompanied by a slight distortion from planarity of the six-membered chelation ring, as P1 deviates by 0.14 Å from the ring plane. The [Ru(Haidf)]$^+$ cations are assembled in dimeric units (Figure 5) by N–H···Cl hydrogen bonds [N2···Cl(ii): 3.300(6) Å, N2–H···Cl(ii): 149(7)°,

Table 2. Bond lengths [Å] and angles [°] for compounds **4**, **6**, **12**·dmso·H_2O, **15**·1.5$CHCl_3$, with standard uncertainties in parentheses. In **15**·1.5$CHCl_3$ C_T denotes the centroid of the *p*-cymene ring.

Compound **4**					
Ru–N(3)	1.995(2)	P(1)–C(1)	1.845(2)	N(1)–Ru–P(2)	166.42(4)
Ru–N(1)	2.075(1)	C(1)–C(6)	1.405(3)	O(1)–Ru–P(2)	89.30(4)
Ru–O(1)	2.118(1)	C(6)–C(7)	1.457(3)	P(1)–Ru–P(2)	100.60(2)
Ru–P(1)	2.2950(5)	N(3)–Ru–N(1)	89.26(6)	N(3)–Ru–Cl	171.58(5)
Ru–P(2)	2.3688(5)	N(3)–Ru–O(1)	84.94(6)	N(1)–Ru–Cl	85.66(4)
Ru–Cl	2.4222(5)	N(1)–Ru–O(1)	77.13(5)	O(1)–Ru–Cl	87.368(4)
N(1)–C(7)	1.290(2)	N(3)–Ru–P(1)	90.07(5)	P(1)–Ru–Cl	96.89(2)
N(1)–N(2)	1.406(2)	N(1)–Ru–P(1)	92.97(4)	P(2)–Ru–Cl	93.25(2)
N(2)–C(8)	1.310(3)	O(1)–Ru–P(1)	168.94(4)		
O(1)–C(8)	1.295(2)	N(3)–Ru–P(2)	90.10(5)		
Compound **6**					
Ru–N(3)	2.001(6)	P(1)–C(1)	1.845(6)	N(1)–Ru–P(2)	165.2(1)
Ru–N(1)	2.073(5)	C(1)–C(6)	1.410(9)	O(1)–Ru–P(2)	87.8(1)
Ru–O(1)	2.147(4)	C(6)–C(7)	1.44(1)	P(1)–Ru–P(2)	103.48(6)
Ru–P(1)	2.278(2)	N(3)–Ru–N(1)	87.0(2)	N(3)–Ru–Cl	172.2(2)
Ru–P(2)	2.385(2)	N(3)–Ru–O(1)	84.9(2)	N(1)–Ru–Cl	86.7(1)
Ru–Cl	2.398(2)	N(1)–Ru–O(1)	77.6(2)	O(1)–Ru–Cl	89.2(1)
N(1)–C(7)	1.277(8)	N(3)–Ru–P(1)	89.0(2)	P(1)–Ru–Cl	95.72(6)
N(1)–N(2)	1.411(7)	N(1)–Ru–P(1)	91.3(1)	P(2)–Ru–Cl	90.47(6)
N(2)–C(8)	1.325(8)	O(1)–Ru–P(1)	167.6(1)		
O(1)–C(8)	1.241(7)	N(3)–Ru–P(2)	94.4(2)		
Compound **12**·dmso·H_2O					
Ru–N(3)	2.030(3)	N(2)–C(8)	1.316(4)	N(1)–Ru–O(2)	95.6(1)
Ru–N(1)	2.034(3)	N(3)–C(33)	1.288(4)	O(1)–Ru–O(2)	80.65(9)
Ru–O(1)	2.109(2)	N(3)–N(4)	1.419(4)	N(3)–Ru–P(1)	94.58(8)
Ru–O(2)	2.120(2)	N(4)–C(34)	1.310(4)	N(1)–Ru–P(1)	90.67(8)
Ru–P(1)	2.2503(9)	C(1)–C(6)	1.411(4)	O(1)–Ru–P(1)	166.22(7)
Ru–P(2)	2.2553(9)	C(6)–C(7)	1.463(5)	O(2)–Ru–P(1)	93.35(7)
P(1)–C(1)	1.829(3)	C(27)-C(32)	1.425(4)	N(3)–Ru–P(2)	90.79(8)
P(2)–C(27)	1.826(3)	C(32)–C(33)	1.458(5)	N(1)–Ru–P(2)	94.90(8)
O(1)–C(8)	1.288(4)	N(3)–Ru–N(1)	171.9(1)	O(1)–Ru–P(1)	93.28(7)
O(2)–C(34)	1.292(4)	N(3)–Ru–O(1)	96.3(1)	O(2)–Ru–P(2)	166.49(7)
N(1)–C(7)	1.292(4)	N(1)–Ru- = (1)	77.7(1)	P(1)–Ru–P(2)	90.05(3)
N(1)–N(2)	1.409(3)	N(3)–Ru–O(2)	78.0(1)		
Compound **15**·1.5$CHCl_3$					
Ru–C_T	1.698(1)	P–C(21)	1.857(9)	C_T–Ru–P	132.3(1)
Ru–C(31)	2.27(2)	N(1)–C(7)	1.231(16)	C_T–Ru–Cl(2)	125.6(1)
Ru–C(28)	2.28(2)	N(1)–N(2)	1.39(2)	P–Ru–Cl(2)	85.0(2)
Ru–P	2.374(5)	N(2)–C(8)	1.31(3)	C_T–Ru–Cl(1)	124.3(1)
Ru–Cl(2)	2.380(4)	O–C(8)	1.26(3)	P–Ru–Cl(1)	89.1(2)
Ru–Cl(1)	2.422(5)	C(1)–C(6)	1.35(2)	Cl(2)–Ru–Cl(1)	86.0(1)
P–C(1)	1.81(2)	C(6)–C(7)	1.47(2)		

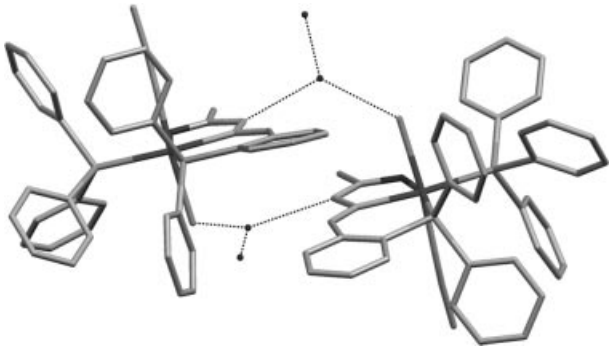

Figure 2. Association in dimers bridged by hydrogen-bonded water molecules in the crystal structure of **4**.

ii: $1-x$, $-y$, $1-z$]; this arrangement recalls the one observed in **4**, where the insertion of a water molecule provides the bridging element, here constituted by the protonated –NH. In the case of **6** the dimer is centrosymmetric.

Repeated attempts aimed at obtaining the dicationic complexes of the type $[Ru(\kappa^3\text{-}(H)PNO)(PPh_3)(CH_3CN)_2][X_2]$ by removal of the second chloride from the complexes **5**–**8** using several halogen scavengers such as KPF_6, $NaBPh_4$, $AgCF_3SO_3$ and $TlPF_6$, have failed due to extensive decompositions or isolation of unknown products, irrespective of the amount of scavenger employed.

However, bis-acetonitrile Ru complexes have been obtained by treatment of the cationic mono-chloride complexes **6** and **7** with an excess of Et_3N in the presence of

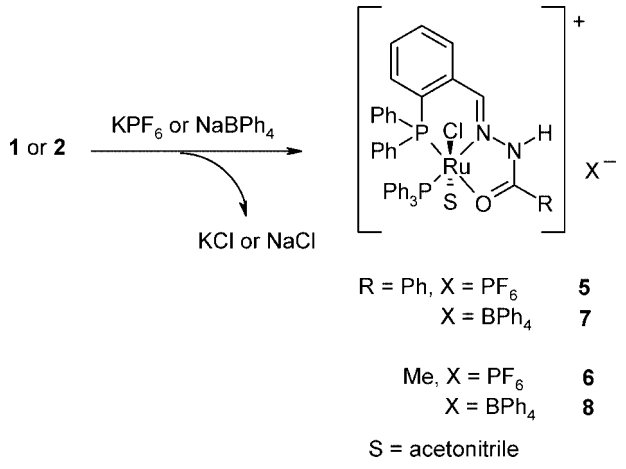

Scheme 6.

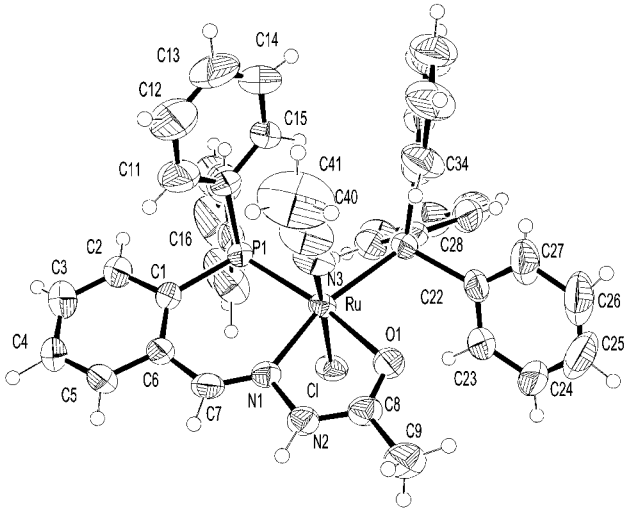

Figure 3. Perspective view and labelling scheme of compound **6**. Rings C16–C21, C28–C33 and C34–C39 are labelled only on the *ipso* carbon for clarity. Thermal ellipsoids at the 50% level. The PF_6^- anion has been omitted.

Figure 4. Superimposition of the molecular structure of **4** ($aidf^-$, grey) and **6** (Haidf, black) showing the geometric effects due to protonation of the PNO ligand.

acetonitrile. This procedure leads to the neutral complexes *trans*-[Ru(κ^3-PNO)(PPh_3)(CH_3CN)$_2$][X] [PNO = bidf, X = BPh_4 (**9**); PNO = aidf, X = PF_6 (**10**)] in good yields (Scheme 7).

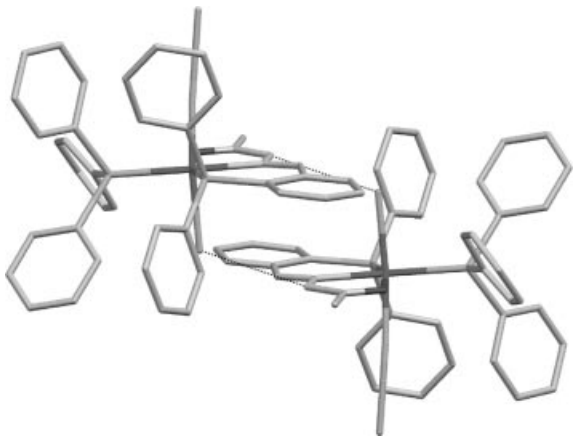

Figure 5. Association in hydrogen-bonded dimers in the crystal structure of **6**.

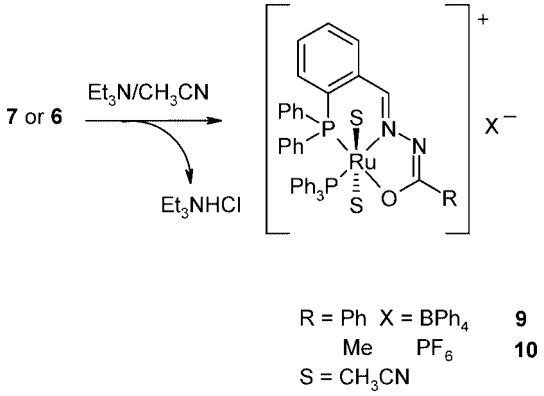

Scheme 7.

The disappearance of the spectroscopic signals of the N–H and C=O bonds agrees with the anionic character of the ligand, while the NMR spectroscopic data similar to those of the precursors indicate that PPh_3 has not moved from its *trans* disposition with respect to the imine moiety (Table 1). The entering of the second molecule of acetonitrile is indicated by ^{1}H NMR spectroscopy with the appearance of an additional singlet at δ = 2.37 and 2.34 ppm for **9** and **10**, respectively. These complexes are significantly unstable both in solution and in the solid state.

Ru Complexes Obtained from [Ru(dmso)$_4$Cl$_2$]

In order to understand the nature of the Ru species involved in the **1** → **12** transformation observed in dmso, the ligand Hbidf has been reacted with [Ru(dmso)$_4$Cl$_2$]. In refluxing EtOH/NaOH [Ru(dmso)$_4$Cl$_2$] reacts with a twofold excess of Hbidf leading to the formation of the bis-chelate octahedral complex [Ru(bidf)$_2$] (**12**) in good yield (Scheme 8). In complex **12** two deprotonated ligands coordinate Ru in a PNO fashion.

The disappearance of the spectroscopic signals of the N–H and C=O bonds is indicative of the deprotonation that occurred in both ligands, while the presence of a singlet at δ = 57.7 ppm in the ^{31}P{^{1}H}-NMR spectrum is in agree-

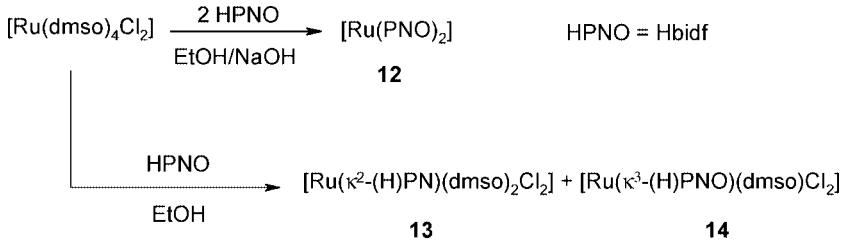

Scheme 8.

ment with two magnetically equivalent phosphorus nuclei. The HC=N proton resonates as a singlet at δ = 9.18 ppm in the ^{1}H NMR spectrum recorded in $CDCl_3$, as expected in the absence of a PPh_3 ligand. The CI-MS spectrum exhibits a cluster centred at *m/z* = 916 (molecular peak). The structure of **12** has been unequivocally established by X-ray diffraction analysis on a single crystal obtained from a dmso solution of **13** (vide infra) and is shown in Figure 6. Compound **12** crystallises as a 1:1:1 dmso/H_2O solvate. The principal geometric features are reported in Table 2. The most relevant feature in the geometry of [Ru(bidf)$_2$] is that the steric hindrance due to the bis-chelation produces significant distortions in the planarity of the two coordinated [PNO] ligands. In fact in both ligands the P atom deviates remarkably from the chelation plane (0.64 and 0.59 Å, respectively), and the Ru–P distances are significantly shorter [Ru–P1: 2.2503(9), Ru–P2: 2.2553(9) Å] than in the previous mono-chelated complexes (Table 2). By contrast, the five-membered chelation rings are planar within 0.09 Å, and the bond lengths along the ring are in agreement with those observed in the neutral mono-chelate **4**. The mutual arrangement of the two ligands in **12**·dmso·H_2O favours a remarkable intramolecular π–π stacking between the rings belonging to the ligands main backbone and the diphenylphosphane rings, with C···C separation ranging between 3.3 and 3.9 Å.

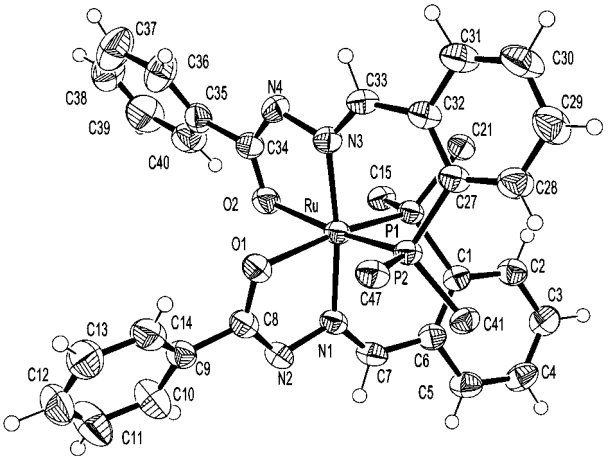

Figure 6. Perspective view and labelling scheme of compound **12**·dmso·H_2O. Rings C15–C20, C21–C26, C41–C46 and C47–C52 are represented only by the *ipso* carbon for clarity. Thermal ellipsoids at the 50% level.

The reaction between Hbidf and [Ru(dmso)$_4$Cl$_2$] has been repeated without a base. When the reaction is carried out at room temperature with a Ru/Hbidf = 1:1 molar ratio, a complex mixture of different products forms, whose separation and identification has not been possible so far. A clearer picture is instead obtained when the reaction is performed in refluxing ethanol. Two different Ru^{II} complexes, [Ru(κ^2-(H)PN)(dmso)$_2$Cl$_2$] (**13**) and [Ru(κ^3-(H)PNO)-(dmso)Cl$_2$] (**14**) form as shown in Scheme 8. In complex **13** the neutral ligand coordinates the metal in a PN bidentate fashion, as evidenced by IR [ν(N–H) = 3249 cm^{-1}, ν(C=O) = 1674 cm^{-1}] and ^{1}HNMR (singlet at δ = 11.24 ppm) spectroscopy.[4] Two chlorides and two dmso molecules complete the octahedron, as evidenced by the IR [two strong bands at 1088 and 1019 cm^{-1} due to the ν(S=O) and δ(C–H), respectively] and ^{1}H NMR (four singlets in the region 3.65–2.84 ppm) spectra as well as by microanalysis. The ^{31}P{^{1}H}-NMR spectrum shows a singlet at δ = 45.5 ppm. From a dmso solution of **13** crystals suitable for X-ray analysis have been collected. The diffractometric analysis shows the formation of the bis-chelate complex **12**; this further mono-chelate → bis-chelate transformation is not surprising, because compound **13** is structurally similar to **1b**, a proposed intermediate in the dmso-promoted **1** → **12** transformation.

In complex **14** the neutral ligand coordinates in a PNO fashion as clearly indicated by the IR bands of the N–H (3156 cm^{-1}) and C=O (1594 cm^{-1}) groups. The hydrazonic proton gives rise to a singlet at δ = 10.34 ppm in the ^{1}H NMR spectrum recorded in $CDCl_3$, while the ^{31}P{^{1}H}-NMR spectrum shows a singlet at δ = 61 ppm. The octahedron is completed by two chlorides and a dmso molecule, while a half dmso molecule is outside of the coordination sphere [the ^{1}H NMR spectrum recorded in $CDCl_3$ shows four singlets in the region 3.48–2.48 ppm, while the IR spectrum shows strong bands at 1095 and 1023 cm^{-1}, attributable to the ν(S=O) and δ(C–H) of the dmso, respectively]. Owing to the lack of structural information, a detailed stereochemical description of the complexes **13** and **14** is not possible at present.

Ru Complex Obtained from [Ru(*p*-cymene)Cl$_2$]$_2$

[Ru(*p*-cymene)Cl$_2$]$_2$ reacts with Hbidf in chloroform at room temperature, leading to the isolation of [(η^6-*p*-cymene)Ru(κ^1-(H)P)Cl$_2$]·3/2 $CHCl_3$ (**15**), where the ligand uses only the P atom to bind to ruthenium. The pseudo-octahedral coordination is completed by a η^6-coordinated *p*-cymene molecule and by two chloride ligands. The IR

spectrum shows the presence of the N–H and of the C=O groups with two bands at 3311 and 1696 cm^{-1}, respectively. The neutral character of the ligand is further substantiated by ^1H NMR spectroscopy with a singlet at δ = 10.31 ppm; the HC=N proton corresponds to a singlet at δ = 9.08 ppm, while the *p*-cymene protons resonate at the expected chemical shifts (in the range 5.47–5.33 ppm). The $^{31}P\{^1H\}$-NMR spectrum recorded in $CDCl_3$ shows a singlet at δ = 29.6 ppm. The structure of **15** has been unambiguously elucidated by X-ray diffraction analysis conducted on a crystal collected from a chloroform/diethyl ether mixture which was cooled to –20 °C. The molecular structure is reported in Figure 7, and the most important geometric parameters are listed in Table 2. The neutral Hbidf ligand is coordinated to the Ru atom only by the P donor [Ru–P bond 2.376(5) Å], while the remaining potential N and O donors point away from the metal. The NH is instead on the same side as the P atom, in the opposite conformation with respect to the one observed in the tridentate complexes. The Ru centre completes its pseudo-octahedral coordination by two chloride atoms and the η^6-*p*-cymene. The conformation of the neutral ligand allows for a favourable contact between the NH and the CH group and one of the coordinated Cl [(N2)H···Cl1: 2.910(5), (C7)H···Cl1: 2.655(5) Å], thus strongly differentiating the intramolecular environment of the two chloride atoms.

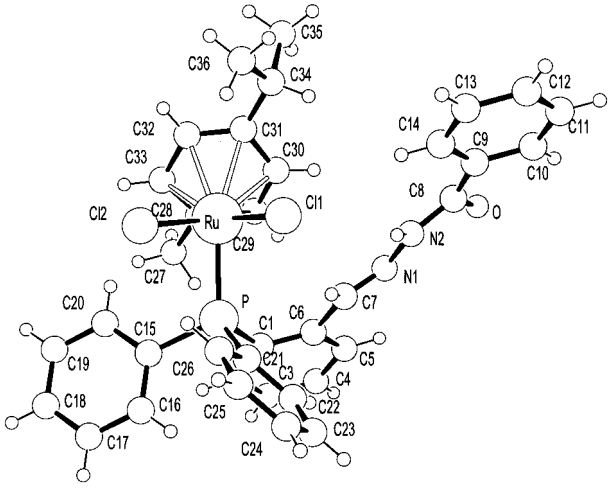

Figure 7. Perspective view and labelling scheme of the ball-and-stick structure of **15**·1.5$CHCl_3$. η^6-Coordination of the *p*-cymene ligand is represented by empty sticks.

Addition of Benzoic Acid to Terminal Alkynes

The Ru-catalysed coupling of alkynes with carboxylic acids (Scheme 2) is an elegant way to obtain enol esters, which are starting materials for several important chemical transformations.[7–13] One of the major goals of this catalysis is the development of stereo- and regio-selective processes leading exclusively to one of the three possible enol ester isomers (Scheme 2), thus the preparation of selective catalysts is certainly desirable. Literature data show that the Markovnikov products are those usually produced using several Ru-catalysts containing monodentate ligands.[15,16a,b,19] However, high selectivity towards (*Z*)-alk-1-en-1-yl benzoate (*anti*-Markovnikov product) has been achieved in the coupling of phenylacetylene with 1-hexyne using allyl–Ru^{II} complexes containing chelating diphosphanes such as dppp or dppb.[16d] The same type of selectivity has been achieved by adding coordinating bases, such as pyridines, to *half-sandwich* Ru^{II} complexes containing monodentate phosphanes,[18] or adding monophosphanes to N-hetherocyclic carbene complexes.[17d] As we wanted to test whether the chelation of the acyl hydrazones could determine a good selectivity towards (*Z*)-alk-1-en-1-yl benzoate, we have tested the complexes **1**–**4**, **6**, **7**, **9** and **10** as pre-catalysts in the addition of benzoic acid to phenylacetylene. To the best of our knowledge, this is the first report dealing with Ru complexes containing tridentate ligands employed as pre-catalysts in such a catalytic transformation. The experimental conditions have been kept constant for every catalytic run: toluene as solvent (for concentrations of about 10^{-3} M all the complexes are perfectly soluble), Na_2CO_3 as base (Ru/base molar ratio = 1:5), T = 120 °C and 1% of catalyst loading. The yields of the reactions (referred to the isolated enol esters) have been checked after 16 hours. The catalytic results are collected in Table 3.

As can be deduced from Entries 1 and 2, the dichloride complexes **1** and **2** are completely inactive in the coupling between 1-hexyne and benzoic acid. This is not unexpected, as it can be imputed to the strongly bound chloride ligands.[8,16a,b,19,34] The substitution of a chloride with a more labile acetonitrile molecule, like in the case of the mono-chloride complexes **3** and **4**, leads to a moderate catalytic activity with 35% and 49% yields (Entries 3 and 4), respectively. However, high stereo- and regio-selectivity in favour of (*Z*)-alk-1-en-1-yl benzoate have been reached in both cases (94% an 99%, respectively). The amount of the Markovnikov product remains very low and no traces of (*E*)-alk-1-en-1-yl benzoate have been detected. The cationic complexes **6** and **7** (Entries 5 and 6) lead to similar yields, but again accompanied by excellent selectivities towards the *Z*-*anti*-Markovnikov product. Finally, the cationic complexes **9** and **10** show catalytic activities comparable to those of the mono-chloride complexes, with a slightly diminished selectivity (10% of the Markovnikov product has been obtained in both cases, Entries 7 and 8). Under the experimental conditions applied, with the only exception of the dichlorides **1** and **2**, the tested Ru complexes result more active than $[Ru(PPh_3)_3Cl_2]$ (Entry 13) which, moreover, leads exclusively to the Markovnikov product. From an inspection of Entries 1–8 of Table 3, it can be inferred that the removal of a chloride ligand is necessary to have catalytic activity accompanied by a good selectivity (compare Entries 1 and 2 with Entries 3 and 4), while the removal of the second chloride ligands does not bring to any improvement of the final yield, but instead provokes a slight decrease in selectivity (compare Entries 3–6 with Entries 7 and 8). The importance of having a vacant coordination site is confirmed by the inertness of the complexes observed in coordinating solvents such as dmso, dmf and acetonitrile;

Table 3. Catalytic results for the addition of benzoic acid to terminal alkynes.[a]

Entry	Ru complex	Alkyne	Yield [%][b]	*Z-anti*-M [%][c]	M [%][c]
1	**1**	1-hexyne	–		
2	**2**	1-hexyne	–		
3	**3**	1-hexyne	35	94	6
4	**4**	1-hexyne	49	99	1
5	**6**	1-hexyne	44	100	–
6	**7**	1-hexyne	53	95	5
7	**9**	1-hexyne	56	90	10
8	**10**	1-hexyne	49	90	10
9	**7**	phenylacetylene	36	81	19
10	**7**	*p*-tolylacetylene	33	98	2
11	**7**	*tert*-butylacetylene	25	86	14
12	**7**	1-octyne	56	94	6
13	$[Ru(PPh_3)_3Cl_2]$	1-hexyne	19	–	100

[a] Conditions: solvent = toluene; T = 120 °C; Ru/benzoic acid/alkyne/Na_2CO_3 = 1:100:100:5. [b] Referred to the isolated product. [c] Determined by ^1H NMR spectroscopy.

no traces of enol esters have been detected even after 24 hours of reaction. From the lengthening of the Ru–O bond observed in the solid structure of **6** with respect to the same bond length found in **4**, one could expect a higher catalytic activity for the complexes containing protonated ligands, such as **6** and **7**, on the basis of a hemilabile behaviour of the acyl hydrazones, from a κ^3-(H)PNO coordination to a κ^2-(H)PN one. However, these pre-catalysts behave similarly to the complexes containing anionic ligands **3**, **4**, **9** and **10**, and this suggests that the acyl hydrazones remain tridentate throughout the catalytic cycle. An explanation of this levelling effect could certainly reside in the deprotonation of the ligand induced by the excess of Na_2CO_3 which forces the acyl hydrazones to an anionic PNO coordination in all cases.

The study of the catalytic behaviour of complex **7** has been extended to other terminal alkynes, such as 1-octyne, phenylacetylene, *p*-tolylacetylene and *tert*-butylacetylene.

Whereas with 1-octyne the catalytic performance is similar to the one observed with 1-hexyne (56% conversion with 94% of *Z-anti*-Markovnikov product and 6% of Markovnikov product, Entry 12), conversions not higher than 36% and lower selectivities have been obtained with the aryl alkynes, (Entries 9 and 10) and with the bulkier *t*Bu-acetylene (Entry 11). Whilst with *t*Bu-acetylene the lower yield can be imputed to steric factors, more difficult is to explain the lower reactivity of the aryl alkynes. Noteworthy is the fact that traces of dimerisation products have been detected neither with phenylacetylene nor with *p*-tolylacetylene, as instead described with Ru–alkylidene complexes bearing N-heterocyclic carbene ligands.[17c] A possible explanation could reside in the bulkiness of the phenyl ring attached to the triple C–C bond of the alkyne which hampers the vinylidene formation (vide infra), but elucidation of this point needs further studies.

ESI-MS Study

ESI-MS technique has been successfully employed in several metal-catalysed transformations like, for example, reduction of ketones,[20] epoxidations,[21] olefins polymerisation[22] and C–H bonds activation[23] for the detection of the metal-containing intermediates involved in the catalytic cycles. To the best of our knowledge, no report dealing with the use of such a technique for the study of the addition of carboxylic acids to alkynes has appeared in the literature. Mechanistic studies conducted on diphosphanes containing complexes,[15d] have evidenced the formation of a vinylidene intermediate as active catalyst, which undergoes an intermolecular attack of a carboxylate anion to generate the final enol ester. We have therefore undertaken an ESI-MS study aimed at detecting the key intermediates involved in the enol ester synthesis catalysed by our Ru–PNO complexes; complex **5** $[Ru(Hbidf)(PPh_3)(CH_3CN)Cl][PF_6]$ has been chosen as a model. Initially, we have collected the ESI(+) spectrum of a 10^{-3} M toluene solution of **5** at room temperature; this shows a predominant cluster centred at m/z = 813 accounting for $[Ru(bidf)(PPh_3)(CH_3CN)]^+$, and minor clusters at m/z = 849 and m/z = 772 accounting for $[Ru(Hbidf)(PPh_3)(CH_3CN)Cl]^+$ and $[Ru(bidf)(PPh_3)]^+$, respectively. The solution has then been heated at 120 °C for 40 minutes and a new ESI(+) spectrum has been collected. This shows again the clusters centred at m/z = 813 and 772, indicating that the complex is preserved under these conditions (Figure 8, a). A small cluster at m/z = 917 shows the presence of **12**, although the isotope pattern points out the presence of a second unknown species with similar mass which tangles the signal up.

To a freshly prepared toluene solution of **5** heated at 120 °C benzoic acid and Na_2CO_3 have been added (Ru/acid/Na_2CO_3 = 1:5:5 molar ratio); the ESI(+) spectrum shows the disappearance of the signal at m/z = 813 in favour of a cluster centred at m/z = 894 corresponding to the fragment $[Ru(Hbidf)(PPh_3)(C_6H_5COO)]^+$, where a carboxylate anion is coordinated to Ru; the clusters at m/z = 772 and 917 are still visible (Figure 8, b). Subsequently, to a freshly prepared toluene solution of **5** heated at 120 °C 1-hexyne has been added (Ru/alkyne = 1:5 molar ratio); the collected ESI(+) spectrum shows the disappearance of the signal at m/z = 813 and the appearance of a cluster at m/z = 854, corresponding to $[Ru(bidf)(PPh_3)(C{=}CH{-}C_4H_9)]^+$ (Figure 8, c); the cluster at m/z = 800 can be tentatively assigned

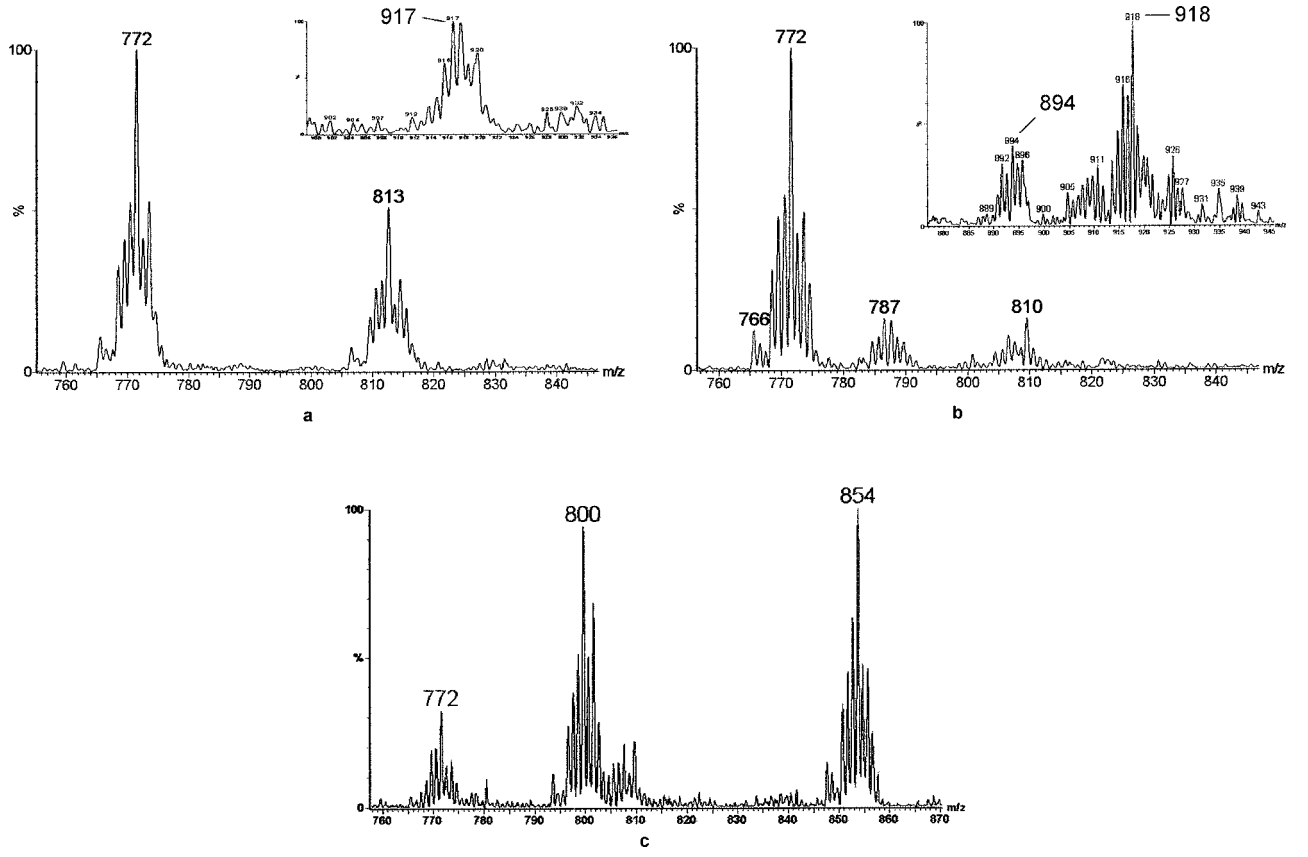

Figure 8. ESI(+) spectra of toluene solutions of **5**: **a**) after one hour at 120 °C; **b**) after the addition of benzoic acid/Na_2CO_3; **c**) after the addition of 1-hexyne.

to the loss of butadiene from the vinylidene species, with formation of the cation $[Ru(bidf)(PPh_3)(C_2H_4)]^+$. This last signal however quickly disappears leaving the signal at *m*/*z* = 854. The formation of the vinylidene intermediate is then independent from the presence of benzoic acid. In fact, the addition of 1-hexyne to a toluene solution containing the carboxylate intermediate leads to the immediate disappearance of the signal at *m*/*z* = 894 in favour of that at *m*/*z* = 854. Although the ESI-MS experiments does not give conclusive evidences of the reaction mechanism governing the studied catalytic process, several observations are in favour of the intermolecular nucleophilic attack of the carboxylate anion onto the vinylidene complex $[Ru(bidf)(PPh_3)(C{=}CH{-}C_4H_9)Cl]$, such as: *i*) the formation of the vinylidene intermediate which occurs independently on the presence of the carboxylate ion, *ii*) that the signal of the carboxylate complex quickly disappears in favour of that of the vinilydene intermediate after the addition of the alkyne, and *iii*) that no signal deriving from vinylidene species containing a carboxylate anion has been detected. Unfortunately, repeated attempts aimed at the isolation or detection of $[Ru(PNO)(PPh_3)(C{=}CH{-}C_4H_9)Cl]$ species have been so far unsuccessful.

The observation of ESI-MS signals attributable to the bis-chelate complex **12** can be one of the reasons of the incomplete conversion of the alkyne substrates, as its formation, through a not defined pathway, can in principle account for catalyst deactivation.

Conclusions

In this work we have reported the synthesis and the full characterisation of several new octahedral Ru^{II} complexes obtained by reaction of $[Ru(PPh_3)_3Cl_2]$ with two protic [PNO] ligands. Depending on the experimental conditions, different coordination modes to Ru can be created, giving rise to neutral or cationic complexes of general formula *trans*-$[Ru(\kappa^3\text{-HPNO})(PPh_3)Cl_2]$, $[Ru(\kappa^3\text{-PNO})(PPh_3)(CH_3CN)Cl]$, $[Ru(\kappa^3\text{-HPNO})(PPh_3)(CH_3CN)Cl][X]$ (X = PF_6 or BPh_4) and $[Ru(\kappa^3\text{-PNO})(PPh_3)(CH_3CN)_2][X]$. The complexes of the type *trans*-$[Ru(\kappa^3\text{-HPNO})(PPh_3)Cl_2]$ show an interesting reactivity with dmso which leads to the formation of bis-chelate complexes of the type $[Ru(\kappa^3\text{-PNO})_2]$. Such unusual conversion, monitored by $^{31}P\{^1H\}$ spectroscopy, occurs through the stepwise decoordination of the three donors of the [PNO] ligand induced by dmso. Then, the initial detachment of the amide oxygen leads to the formation of intermediate species where the ligands are κ^2-(H)PN coordinated; subsequently, the nitrogen decoordination leads to P-monodentate behaviour and, finally, a PNO ligand transfer from two different ruthenium atoms takes

place with formation of the bis-chelate complex [Ru(κ^3-PNO)$_2$], [Ru(dmso)$_4$Cl$_2$], Me_2S, $OPPh_3$ and HCl. The deoxygenation of dmso occurs by oxygen transfer to a PPh_3 molcule. Model systems of the spectroscopically detected intermediates have been obtained by reaction of an HPNO ligand with [Ru(dmso)$_4$Cl$_2$] and [Ru(*p*-cymene)Cl$_2$]$_2$. A catalytic version of the oxygen transfer reaction from dmso to PPh_3 has also been developed.

Most of the complexes containing PPh_3 promote the catalytic coupling between benzoic acid and terminal alkynes in toluene/Na_2CO_3 at 120 °C, with 1% of catalyst loading. The reactions proceed with high stereo- and regioselectivity, up to 100% as established by ^{1}HNMR, towards the formation of the *anti*-Markovnikov product. Important mechanistic details come from the ESI-MS study applied for the first time to this ruthenium-catalysed coupling reaction: the enol esters form thanks to an intermolecular nucleophilic attack of a uncoordinated carboxylate anion onto a Ru–vinylidene intermediate of the type [Ru(PNO)(PPh_3)(C=CH–C_4H_9)Cl].

Experimental Section

General: All reactions were performed under dry nitrogen employing standard Schlenk techniques. Solvents were dried prior to use and stored under nitrogen. Elemental analysis (C, H, N and S) were performed with a Carlo Erba Mod. EA 1108 apparatus. Infrared spectra were recorded with a Nicolet 5PCFT-IR spectrophotometer in the 4000–400 cm^{-1} range by using KBr disks. ^{1}H NMR spectra were obtained with a Bruker 300 FT spectrometer using $SiMe_4$ as internal standard, while ^{31}P{^{1}H} NMR spectra were recorded with a Bruker AMX 400 FT using H_3PO_4 85% as external standard. Heterocorrelated ^{31}P-^{1}H NMR spectra were measured with a Bruker Avance 400 MHz. All spectra were collected at 298 K. FAB-MS spectra were performed with a Micromass Autoespec mass spectrometer, employing *m*-nitrobenzyl alcohol as matrix. A Quattro LC triple quadrupole instrument (Micromass, Manchester, UK) equipped with an electrospray interface and a Masslynx v. 3.4 software (Micromass) was used for ESI-MS data acquisition and processing. The nebulizing gas (nitrogen, 99.999% purity) and the desolvation gas (nitrogen, 99.998% purity) were delivered at a flow-rate of 80 and 500 L/h, respectively. ESI-MS analyses were performed by operating the mass spectrometer in positive (PI) ion mode, acquiring mass spectra over the scan range *m*/*z* 100–1300, using a step size of 0.1 Da and a scan time of 1.2 seconds. The operating parameters of the interface were as follows: source temperature 70 °C, desolvation temperature 70 °C, ES(+) voltage 3.0 kV, cone voltage 30 and 50 V, rf lens 0.3 V.

2-(Diphenylphosphanyl)benzaldehyde benzoylhydrazone (**Hbidf**) and 2-(diphenylphosphanyl)benzaldehyde acetylhydrazone (**Haidf**) were synthesised as previously reported.[4b] [Ru(PPh_3)$_3$Cl$_2$] was synthesised by a literature reported method.[35]

***trans*-[Ru(Hbidf)(PPh_3)Cl$_2$]·CH_2Cl_2 (1):** The ligand (250 mg, 0.613 mmol) was dissolved in 15 mL of CH_2Cl_2 at room temperature. After 10 minutes of stirring [Ru(PPh_3)$_3$Cl$_2$] (590 mg, 0.617 mmol) was added and the resulting purple solution was stirred for 5 hours at room temperature. The solvent was partially removed in vacuo, and the solution was cooled to –18 °C for a night. A purple powder was filtered off, washed with *n*-hexane and diethyl ether and then dried under vacuum. Yield: 430 mg (83%). M.p. 160 °C (dec.). $C_{44}H_{36}Cl_2N_2OP_2Ru$·$CH_2Cl_2$ (927.642): calcd. C 58.25, H 4.10, N 3.02; found C 58.85, H, 4.11, N 3.02. ^{1}H NMR ([D$_6$]dmso): δ = 8.02–6.94 (m, 34 H, Ph), 5.20 (s, 2 H, CH_2Cl_2) ppm. FAB-MS: *m*/*z* = 842 [M – CH_2Cl_2]$^+$, 807 [M – CH_2Cl_2 – Cl]$^+$.

***trans*-[Ru(Haidf)(PPh_3)Cl$_2$]·1/2 CH_2Cl_2 (2):** As for **1** but using ligand **Haidf** (150 mg, 0.433 mmol). Yield: 310 mg (91%). M.p. 160 °C (dec.). $C_{39}H_{34}Cl_2N_2OP_2Ru$·1/2$CH_2Cl_2$ (823.105): calcd. C 57.75, H 4.26, N 3.41; found C 58.38, H 4.16, N 3.40. ^{1}H NMR ([D$_6$]dmso): δ = 7.75–6.87 (m, 29 H, Ph), 5.21 (s, 1 H, CH_2Cl_2), 2.25 [s, 3 H, CH_3C(O)] ppm. FAB-MS: *m*/*z* = 780 [M – CH_2Cl_2 + H$^+$]$^+$, 745 [M – CH_2Cl_2 – Cl]$^+$, 709 [M – CH_2Cl_2 – HCl – Cl]$^+$.

[Ru(bidf)(PPh_3)(CH_3CN)Cl] (3): Complex **1** (320 mg, 0.380 mmol) was dispersed in 20 mL of toluene at room temperature. NEt_3 (262 μL, 1.900 mmol) and CH_3CN (1 mL) were added, and the purple solution was stirred at room temperature overnight. A yellow solid was filtered off, washed with water and *n*-hexane and then dried under vacuum. Yield: 260 mg (81%). M.p. 180 °C (dec.). $C_{46}H_{41}ClN_3OP_2Ru$ (850.325): calcd. C 62.25, H 4.52, N 4.96; found C 65.90, H 4.98, N 4.65. ^{1}H NMR (CD_2Cl_2): δ = 8.16 (dd, 2 H, Ph), 7.30 (t, 2 H, Ph), 7.28–7.14 (m, 28 H, Ph), 7.12 (t, 1 H, Ph), 6.58 (t, 2 H, Ph), 1.21 (s, 3 H, CH_3CN) ppm. FAB-MS: *m*/*z* = 806 [M – CH_3CN]$^+$, 771 [M – CH_3CN – Cl]$^+$.

[Ru(aidf)(PPh_3)(CH_3CN)Cl] (4): As for **3** but starting from complex **2**. Yellow solid. Yield: 130 mg (81%). M.p. 174 °C (dec.). $C_{41}H_{36}ClN_3OP_2Ru$ (785.23): calcd. C 62.86, H 4.60, N 5.36; found C 62.98, H 4.75, N 4.95. ^{1}H NMR (CD_2Cl_2): δ = 7.80 (t, 2 H, Ph), 7.58–7.11 (m, 24 H, Ph), 6.95 (t, 1 H, Ph), 6.54 (t, 2 H, Ph), 2.36 [s, 3 H, CH_3C(O)], 1.21 (s, 3 H, CH_3CN) ppm. FAB-MS: *m*/*z* = 786 [M + H$^+$]$^+$, 744 [M – CH_3CN]$^+$. For slow evaporation of a dichloromethane/acetonitrile mixture, crystals suitable for X-ray analysis were collected.

[Ru(Hbidf)(PPh_3)(CH_3CN)Cl][PF_6] (5): Complex **1** (250 mg, 0.297 mmol) was dispersed in 45 mL of CH_2Cl_2 at room temperature. After 15 minutes of stirring KPF_6 (280 mg, 1.521 mmol) and CH_3CN (1 mL) were added. The solution was stirred overnight at room temperature, then filtered and the resulting orange solution was concentrated under vacuum, treated with *n*-hexane and refrigerated at –18 °C. An orange powder was filtered off, washed with *n*-hexane and dried under vacuum. Yield: 210 mg (71%). M.p. 170 °C (dec.). $C_{46}H_{39}ClF_6N_3OP_3Ru$ (993.271): calcd. C 55.65, H 3.93, N 4.23; found C 55.34, H 3.89, N 4.31. IR (cm^{-1}): $\tilde{\nu}$ = 2281 (w, $CH_3C{\equiv}N$), 845 (vs, PF). ^{1}H NMR (CD_2Cl_2): δ = 8.01 (d, 2 H, Ph), 7.70 (m, 1 H, Ph), 7.63–7.23 (m, 28 H, Ph), 7.18 (t, 1 H, Ph), 6.40 (t, 2 H, Ph), 1.63 (s, 3 H, CH_3CN) ppm. ^{31}P{^{1}H}NMR (CD_2Cl_2): δ = –141.1 (m, 1 P, PF_6) ppm. FAB-MS: *m*/*z* = 806 [M – PF_6 – CH_3CN]$^+$, 771 [M – PF_6 – CH_3CN – HCl]$^+$.

[Ru(Haidf)(PPh_3)(CH_3CN)Cl][PF_6]·CH_2Cl_2 (6): As for **5** but starting from complex **2**. Yield: 160 mg (69%). M.p. 170 °C (dec.). $C_{41}H_{37}ClF_6N_3OP_3Ru$·$CH_2Cl_2$ (1016.133): calcd. C 49.65, H 4.14, N 4.14; found C 50.00, H 3.91, N 4.48. IR (cm^{-1}): $\tilde{\nu}$ = 2273 (w, $CH_3C{\equiv}N$), 845 (vs, PF). ^{1}H NMR (CD_2Cl_2): δ = 8.88 (br., 1 H, CH=N), 7.88 (t, 2 H, Ph), 7.72–7.03 (m, 25 H, Ph), 6.33 (t, 2 H, Ph), 5.20 (s, 2 H, CH_2Cl_2), 2.38 [s, 3 H, CH_3C(O)] 1.70 (s, 3 H, CH_3CN) ppm. ^{31}P{^{1}H}NMR (CD_2Cl_2): δ = –145.5 (m, 1 P, PF_6) ppm. FAB-MS: *m*/*z* = 786 [M – CH_2Cl_2 – PF_6]$^+$, 745 [M – CH_2Cl_2 – PF_6 – CH_3CN]$^+$, 709 [M – CH_2Cl_2 – PF_6 – CH_3CN – HCl]$^+$. From a refrigerated dichloromethane /*n*-pentane mixture, crystals suitable for X-ray analysis were collected.

[Ru(Hbidf)(PPh_3)(CH_3CN)Cl][BPh_4] (7): As for **6** but starting from complex **1** and using $NaBPh_4$ instead of KPF_6. Yield: 180 mg (81%). M.p. 146–148 °C. $C_{70}H_{59}BClN_3OP_2Ru$ (1167.544): calcd. C

72.04, H 5.06, N 3.60; found C 72.45, H 5.74, N 3.48. IR (cm^{-1}): $\tilde{\nu}$ = 2269 (w, $CH_3C{\equiv}N$), 843 (w, BP). ^1H NMR (CD_2Cl_2): δ = 8.03 (d, 2 H, Ph), 7.83–6.84 (m, 50 H, Ph), 6.39 (t, 2 H, Ph), 1.23 (s, 3 H, CH_3CN) ppm. FAB-MS: *m*/*z* = 848 $[M - BPh_4]^+$, 807 $[M - BPh_4 - CH_3CN]^+$, 771 $[M - BPh_4 - CH_3CN - HCl]^+$.

[Ru(Haidf)(PPh$_3$)(CH$_3$CN)Cl][BPh$_4$] (8): As for **7** but starting from complex **2**. Yield: 50 mg (70%). M.p. 152–154 °C. $C_{65}H_{57}BClN_3OP_2Ru{\cdot}1/4CH_2Cl_2$ (1171.747): calcd. C 69.65, H 5.03, N 3.38; found C 69.68, H 5.15, N 3.74. IR (cm^{-1}): $\tilde{\nu}$ = 2265 (w, $CH_3C{\equiv}N$), 851 (w, BP). ^{1}HNMR ($CDCl_3$): δ = 7.83–6.84 (m, 47 H, Ph), 6.53 (t, 2 H, Ph), 2.23 [s, 3 H, $CH_3C(O)$], 0.43 (s, 3 H, $CH_3C{\equiv}N$) ppm. FAB-MS: *m*/*z* = 786 $[M - BPh_4]^+$, 745 $[M - BPh_4 - CH_3CN]^+$, 709 $[M - BPh_4 - CH_3CN - HCl]^+$.

***trans*-[Ru(bidf)(PPh$_3$)(CH$_3$CN)$_2$][BPh$_4$] (9):** Complex **7** (110 mg, 0.094 mmol) was dissolved in 20 mL of tolune at room temperature. To the resulting yellow solution acetonitrile (3 mL) and NEt_3 (75 μL, 0.539 mmol) were added and then it was left stirring at room temperature overnight. The solvent was completely removed under vacuum obtaining a sticky pale orange solid, which was washed with water and repeatedly triturated with *n*-hexane. The bright orange powder was finally filtered off, washed with diethyl ether and dried under vacuum. Yield: 90 mg (82%). M.p. 150–154 °C. Due to the instability of the complex, irreproducible microanalyses have been obtained. IR (cm^{-1}): $\tilde{\nu}$ = 2273 (w, $CH_3C{\equiv}N$), 873 (w, BP). ^{1}H NMR (CD_2Cl_2): δ = 8.21 (d, 2 H, Ph), 7.70 (t, 1 H, Ph), 7.46–7.05 (m, 49 H, Ph), 6.55 (t, 2 H, Ph), 2.37 (s, 3 H, $CH_3C{\equiv}N$), 1.29 (s, 3 H, $CH_3C{\equiv}N$) ppm. FAB-MS: *m*/*z* = 771 $[M - BPh_4 - 2CH_3CN]^+$.

***trans*-[Ru(aidf)(PPh$_3$)(CH$_3$CN)$_2$][PF$_6$] (10):** As for **9** but starting form complex **8**. Yield: 50 mg (76%). M.p. 137–142 °C. Due to the instability of the complex, irreproducible microanalyses have been obtained. IR (cm^{-1}): $\tilde{\nu}$ = 2281 (w, $CH_3C{\equiv}N$), 835 (vs, PF). ^{1}H NMR (CD_2Cl_2): δ = 7.72 (t, 2 H, Ph), 7.61 (t, 2 H, Ph), 7.48–7.12 (m, 22 H, Ph), 7.05 (t, 2 H, Ph), 6.51 (t, 2 H, Ph), 2.34 [s, 3 H, $CH_3C(O)$], 1.44 (s, 3 H, $CH_3C{\equiv}N$), 1.27 (s, 3 H, $CH_3C{\equiv}N$) ppm. $^{31}P\{^1H\}$NMR (CD_2Cl_2): δ = –150 (m, 1 P, PF_6) ppm.

[Ru(Hbidf)(PPh$_3$)(CH$_3$CN)Cl]Cl (11): Complex **1** (100 mg, 0.12 mmol) was treated with CH_3CN and the mixture was heated at 50 °C for 4 hours. The initial purple mixture became an almost clear orange solution. After filtration the resulting orange solution was dried under vacuum, obtaining an orange powder. Yield: 60 mg (57%). $C_{46}H_{37}Cl_2N_3OP_2Ru$ (881.746): calcd. C 62.16, H 4.25, N 4.57; found C 62.38, H 4.46, N 4.57. IR (cm^{-1}): $\tilde{\nu}$ = 2273 (w, $CH_3C{\equiv}N$). ^{1}H NMR (CD_2Cl_2): δ = 7.88–6.86 (m, 32 H, Ph), 6.55 (t, 2 H, Ph), 1.31 (s, 3 H, $CH_3C{\equiv}N$) ppm.

[Ru(bidf)$_2$]·2H$_2$O (12). Method A: Hbidf (100 mg, 0.244 mmol) was dissolved in ethanol (25 mL) by warming. 1 M NaOH solution was added until a pH ≈ 8 (checked by litmus paper), obtaining a pale yellow solution. $[Ru(dmso)_4Cl_2]$ (59.3 mg, 0.122 mmol) was dissolved in ethanol (10 mL) and added to the ligand solution. After 2 h of reflux the solvent was partially removed under vacuum and the resultant clear solution was refrigerated at –20 °C. The soformed solid was filtered off, washed with cold ethanol and vacuum dried. Yield: 84 mg (75%).

Method B: Hbidf (140 mg, 0.343 mmol) was dissolved in 5 mL of CH_2Cl_2 at room temperature. A KOH solution (3.75 mL , 0.21 M) was added, and the resulting pale yellow solution was stirred at room temperature for 1 hour. $[Ru(PPh_3)_3Cl_2]$ (160 mg, 0.167 mmol) previously dissolved in 15 mL of CH_2Cl_2 was added, and the mixture stirred at room temperature for 3 hours. The solution was then filtered and the solvent partially removed under vacuum. After cooling at –18 °C a yellow solid formed, which was filtered off, washed with diethyl ether and vacuum dried. Yield: 99 mg (63%) M.p. 253–258 °C. $C_{52}H_{40}N_4O_2P_2Ru{\cdot}2H_2O$ (951.966): calcd. C 65.60, H 4.65, N 5.88; found C 65.26, H 4.76, N 5.59. ^{1}H NMR ($CDCl_3$): δ = 7.66 (d, 4 H, Ph), 7.19–6.77 (m, 38 H, Ph) ppm. CI-MS: *m*/*z* = 916 $[M - H_2O]^+$.

[Ru(Hbidf)(dmso)$_2$Cl$_2$] (13) and [Ru(Hbidf)(dmso)Cl$_2$]·1/2dmso·H$_2$O (14): $[Ru(dmso)_4]Cl_2$ (59.3 mg, 0.122 mmol) was dissolved in ethanol (15 mL). An equimolar amount of Hbidf dissolved in ethanol (15 mL) was added, and the resulting solution was refluxed for 1 h. A yellow solid precipitated (**13**), which was filtered off, washed with ethanol and vacuum dried for several hours. Yield: 31 mg (35%). M.p. 227 °C (dec.). $C_{30}H_{33}Cl_2N_2O_3PRuS_2$ (736.675): calcd. C 48.91, H 4.51, N 3.80, S, 8.70; found C 48.86, H 4.47, N 3.86; S, 8.78. IR (cm^{-1}): $\tilde{\nu}$ = 1088 (vs, S=O); 1019 (s, $\rho C–H)_{dmso}$. ^{1}H NMR ($CDCl_3$): δ = 7.92 (d, 2 H, Ph), 7.79–7.20 (m, 17 H, Ph), 3.65 (s, 3 H, dmso), 3.45 (s, 3 H, dmso), 3.03 (s, 3 H, dmso), 2.84 (s, 3 H, dmso) ppm. By slow evaporation of a dmso solution of **13** crystals of **12**·dmso·H$_2$O suitable for X-ray analysis were collected (see crystallograhic analysis).

After the filtration of **13**, the resulting solution was treated with *n*-hexane observing the precipitation of an orange solid (**14**), which was filtered off, washed with *n*-hexane and vacuum dried. Yield: 34 mg (40%). M.p. 228 °C (dec.). $C_{29}H_{32}Cl_2N_2O_{3.5}PRuS_{1.5}$ (715.625): calcd. C 48.67, H 4.51, N 3.91, S 6.72; found C 48.21, H 4.71, N 4.22, S 7.14. IR (cm^{-1}): $\tilde{\nu}$ = 1095 (vs, S=O), 1023 (s, $\rho C–H)_{dmso}$. ^{1}H NMR ($CDCl_3$): δ = 7.78–7.35 (m, 19 H, Ph), 3.48 (s, 3 H, dmso), 2.95 (s, 3 H, dmso) ppm.

[Ru(Hbidf)(*p*-cymene)Cl$_2$]·2CHCl$_3$ (15): Hbidf (50 mg, 0.122 mmol) was dissolved in 40 mL of chloroform and $[Ru(p\text{-cymene})Cl_2]_2$ (75 mg, 0.122 mmol) was added. The mixture was stirred at room temperature for 2.5 hours obtaining a deep red solution, which was reduced in volume and treated with diethyl ether. A brown solid precipitated (25 mg) whose characterisation was not possible. From the mother liquors refrigerated at –20 °C, brown crystals suitable for X-ray analysis were collected. Yield: 46.5 mg (40%). M.p. 220 °C (dec.). $C_{36}H_{35}Cl_2N_2OPRu{\cdot}2CHCl_3$ (953.395): calcd. C 47.87, H 3.90, N 2.90; found C 48.20, H 3.80, N 2.30. ^{1}H NMR ($CDCl_3$): δ = 8.07 (d, 2 H, Ph), 7.62–7.03 (m, 17 H, Ph), 5.47 (d, 2 H, *p*-cymene), 5.33 (d, 2 H, *p*-cymene), 2.94 [m, 1 H, C*H*-$(CH_3)_2$], 1.75 [s, 3 H, $CH(CH_3)_2$], 1.28 [s, 3 H, $CH(CH_3)_2$] ppm.

X-ray Analysis: Mo-K_α radiation (λ = 0.71073 Å), T = 293 K, on a SMART AXS 1000 diffractometer equipped with CCD detector was used for compounds **4** and **6** and **12**·dmso·H$_2$O, while Cu-K_α radiation (λ = 1.54178 Å), T = 293 K, with a Siemens AED diffractometer equipped with scintillation detector was employed for **15**·1.5CHCl$_3$, which showed a significant crystal decay over the data collection (47% intensity loss, correction applied). Lorentz, polarisation, and absorption corrections were applied.[36] Structures were solved by direct methods using SIR97[37] and refined by full-matrix least-squares on all F^2 using SHELXL97[38] implemented in the WingX package.[39] Hydrogen atoms were partly located on Fourier difference maps and refined isotropically, partly introduced in calculated positions. Anisotropic displacement parameters were refined for all non-hydrogen atoms in **4**, **6** and **12**·dmso·H$_2$O, but only for Ru and its coordination environment for **15**·1.5CHCl$_3$. In **12**·dmso·H$_2$O the dmso presents a disorder on the S atom. Final geometries have been analysed with SHELXL97[36] and PARST97,[40] and extensive use was made of the Cambridge Crystallographic Data Centre packages.[41] Table 4 summarises crystal data and structure determination results.

Table 4. Crystal data and structure refinement for structure analyses.

	4	**6**	**12**·dmso·H_2O	**15**·1.5 $CHCl_3$
Empirical formula	$C_{41}H_{40}ClN_3O_3P_2Ru$	$C_{41}H_{37}ClF_6N_3OP_3Ru$	$C_{54}H_{48}N_4O_4P_2RuS$	$C_{38}H_{37}Cl_{6.50}N_2OPRu$
Formula weight	821.22	931.17	1012.03	900.16
Wavelength	0.71073 Å	0.71073 Å	0.71073 Å	1.54100 Å
Crystal system	tetragonal	orthorhombic	monoclinic	hexagonal
Space group	$P4_32_12$	*Pcab*	$P2_1/c$	*R*-3
Unit cell dimensions [Å, °]	a = 14.430(1)	a = 18.334(1)	a = 11.114(2)	a = 41.520(8)
	b = 14.430(1)	b = 20.599(1)	b = 21.271(4) β = 95.89(1)	b = 41.520(8)
	c = 37.134(2)	c = 21.621(1)	c = 20.280(4)	c = 13.270(4)
Volume [$Å^3$]	7732.2(9)	8165.4(7)	4769(2)	19811(8)
Z	8	8	4	18
Density (calculated) [mg/m^3]	1.411	1.515	1.410	1.358
Absorption coefficient [mm^{-1}]	0.599	0.631	0.491	7.090
$F(000)$	3376	3776	2088	8217
Θ range for data collection [°]	1.51–27.10	1.76–28.42	1.39–28.49	3.55–64.77
Reflections collected	84143	86434	28916	7243
Independent reflections	8525 [R(int) = 0.0314]	9617 [R(int) = 0.0720]	10731 [R(int) = 0.0523]	6370 [R(int) = 0.0835]
Data/restraints/parameters	8525/6/480	9617/0/615	10731/2/775	6370/5/222
Goodness-of-fit on F^2	1.180	1.203	0.875	0.780
Final R indices [$I > 2\sigma(I)$] (R_1, wR_2)	0.0296, 0.0631	0.0709, 0.1465	0.0454, 0.0963	0.1135, 0.3044
R indices (all data) (R_1, wR_2)	0.0343, 0.0655	0.1205, 0.1593	0.0918, 0.1114	0.2530, 0.3526
Largest ΔF max./min. [e·$Å^{-3}$]	0.472/–0.516	0.539/–0.518	0.981/–0.675	0.964/–0.506

CCDC-294363 (for **4**), -294364 (for **6**), -294365 (for **12**·dmso·H_2O) and -294366 (for **15**·1.5 $CHCl_3$) contain the supplementary crystallographic data for this paper. These data can be obtained free of charge from The Cambridge Crystallographic Data Centre via www.ccdc.cam.ac.uk/data_request/cif.

Catalytic Reactions

Addition of Benzoic Acid to Terminal Alkynes: A toluene solution (7 mL) containing the catalyst (0.01 mmol) and the alkyne (1 mmol) was added at room temperature to a toluene solution (6 mL) of benzoic acid containing solid Na_2CO_3 (0.05 mmol). The resulting mixture was heated to 120 °C and stirred for 16 hours, then dried under vacuum; the residual solid was treated with 5 mL of CH_2Cl_2 and the precipitate was filtered off. Solid $NaHCO_3$ (1 mmol) was added, and the mixture was washed with H_2O three times; the organic layer was dried by anhydrous Na_2SO_4 and reduced in volume by vacuum and then filtered through silica gel to remove the catalyst. The solution was finally dried under vacuum and analysed by ^1H NMR spectroscopy.

Oxygen Transfer from Dmso to PPh_3: Compound **1** (11 mg, 0.012 mmol) was dissolved in 8 mL of nitrogen-saturated dmso and PPh_3 (326 mg, 1.243 mmol) was added. The yellow solution was refluxed under nitrogen and small samples were withdrawn at regular intervals, added of $CDCl_3$ and analysed by $^{31}P\{^1H\}$-NMR spectroscopy.

Supporting Information (see footnote on the first page of this article): $^{31}P\{^1H\}$-NMR spectra of complex **1** recorded in [D_6]dmso.

Acknowledgments

Dr P. Barbaro (ICCOM-CNR) is gratefully thanked for running the heterocorrelated ^{31}P-^1H spectra, while Dr. Maria Carmen Rodriguez Argüelles (University of Vigo, Spain) is thanked for FAB-MS measurements. SB thanks Xunta de Galicia for a postdoctoral grant. The authors thank ECRF and "Firenze Hydrolab" Project for access to Bruker Avance 400 MHz and the Centro Interfacoltà di Misure G. Casnati of the University of Parma for the instrument facilities.

[1] a) M. Alvarez, N. Lugan, R. Mathieu, *J. Chem. Soc., Dalton Trans.* **1994**, 2755–2760; b) J. R. Dilworth, S. D. Howe, A. J. Hutson, J. R. Miller, J. Silver, R. M. Thompson, M. Harman, M. B. Hursthouse, *J. Chem. Soc., Dalton Trans.* **1994**, 3553–3562; c) K. K. Hii, S. D. Perera, B. L. Shaw, *J. Chem. Soc., Dalton Trans.* **1994**, 3589–3596; d) P. Bhattacharyya, J. Parr, A. M. Z. Slawin, *J. Chem. Soc., Dalton Trans.* **1998**, 3609–3614; e) P. Bhattacharyya, M. L. Loza, J. Parr, A. M. Z. Slawin, *J. Chem. Soc., Dalton Trans.* **1999**, 2917–2921; f) J. D. G. Correia, A. Domingos, A. Paulo, I. Santos, *J. Chem. Soc., Dalton Trans.* **2000**, 2477–2482; g) J. W. Faller, G. Mason, J. Parr, *J. Organomet. Chem.* **2001**, *626*, 181–185; h) K. Nakajima, S. Ishibashi, M. Inamo, M. Kojima, *Inorg. Chim. Acta* **2001**, *325*, 36–44; i) G. Sanchez, F. Momblona, J. L. Serrano, L. Garcia, E. Perez, J. Perez, G. Lopez, *J. Coord. Chem.* **2002**, *55*, 917–923; j) M. Ahmad, S. D. Perera, B. L. Shaw, M. Thornton-Pett, *J. Chem. Soc., Dalton Trans.* **2002**, 1954–1962; k) S. R. Korupoju, R.-Y. Lai, Y.-H. Liu, S.-M. Peng, S.-T. Liu, *Inorg. Chim. Acta* **2005**, *358*, 3003–3008.

[2] a) H. Yang, M. Alvarez, N. Lugan, R. Mathieu, *J. Chem. Soc., Chem. Commun.* **1995**, 1721–1722; b) H. Yang, M. Alvarez-Gressier, N. Lugan, R. Mathieu, *Organometallics* **1997**, *16*, 1401–1409; c) H. L. Kwong, W. S. Lee, T. S. Lai, W. T. Wong, *Inorg. Chem. Commun.* **1999**, *2*, 66–69; d) H. Dai, X. Hu, H. Chen, C. Bai, Z. Zheng, *Tetrahedron: Asymmetry* **2003**, *14*, 1467–1472.

[3] P. Pelagatti, A. Bacchi, M. Carcelli, M. Costa, A. Fochi, P. Ghidini, E. Leporati, M. Masi, C. Pelizzi, G. Pelizzi, *J. Organomet. Chem.* **1999**, *583*, 94–105.

[4] a) A. Bacchi, M. Carcelli, M. Costa, P. Pelagatti, C. Pelizzi, G. Pelizzi, *Gazz. Chim. Ital.* **1994**, *124*, 429–435; b) A. Bacchi, M. Carcelli, M. Costa, A. Leporati, E. Leporati, P. Pelagatti, C. Pelizzi, G. Pelizzi, *J. Organomet. Chem.* **1997**, *535*, 107–120.

[5] a) P. Pelagatti, A. Bacchi, C. Bobbio, M. Carcelli, M. Costa, C. Pelizzi, C. Vivorio, *Organometallics* **2000**, *19*, 5440–5446; b) P. Pelagatti, A. Bacchi, C. Bobbio, M. Carcelli, M. Costa, A. Fochi, C. Pelizzi, *J. Chem. Soc., Dalton Trans.* **2002**, 1–7; c) P. Pelagatti, A. Bacchi, M. Carcelli, M. Costa, H.-W. Frühauf, K. Goubitz, C. Pelizzi, M. Triclistri, K. Vrieze, *Eur. J. Inorg. Chem.* **2002**, 439–446.

[6] C. Bruneau, P. H. Dixneuf, *Ruthenium Catalysts and Fine Chemistry*, Springer GmbH, Berlin, Germany, **2004**.

[7] J. P. Monthéard, M. Camps, G. Seytre, J. Guillet, J. C. Dubois, *Angew. Makromol. Chem.* **1978**, *72*, 45–55.
[8] E. Bruneau, M. Neveux, Z. Kabouche, C. Ruppin, P. H. Dixneuf, *Synlett* **1991**, 755–763.
[9] a) R. C. Cambie, R. C. Hayward, J. L. Jurlina, P. S. Rutledge, P. D. Woodgate, *J. Chem. Soc., Perkin Trans. 1* **1978**, 126–130; b) S. Torii, T. Inokuchi, S. Misima, T. Kobayashi, *J. Org. Chem.* **1980**, *45*, 2731–2735; c) S. Stavber, B. Sket, B. Zajc, M. Zupan, *Tetrahedron* **1989**, *45*, 6003–6010; d) A. D. Cort, *J. Org. Chem.* **1991**, *56*, 6708–6709.
[10] a) A. Demonceau, E. Saive, Y. de Froidmont, A. F. Noels, A. J. Hubert, *Tetrahedron Lett.* **1992**, *33*, 2009–2012; b) W. B. Motherwell, L. R. Roberts, *J. Chem. Soc., Chem. Commun.* **1992**, 1582–1583.
[11] a) L. F. Tietze, A. Montenbruck, C. Schneider, *Synlett* **1994**, 509–510; b) M. C. Pirrung, Y. R. Lee, *Tetrahedron Lett.* **1994**, *35*, 6231–6234.
[12] K. E. Koenig, G. L. Bachman, B. E. Vineyard, *J. Org. Chem.* **1980**, *45*, 2362–2365.
[13] a) N. Sakai, K. Nozaki, K. Massima, H. Takaya, *Tetrahedron: Asymmetry* **1992**, *3*, 583–586; b) C. G. Arena, F. Nicolò, D. Drommi, G. Bruno, F. Faraone, *J. Chem. Soc., Chem. Commun.* **1994**, 2251–2252.
[14] M. Rotem, Y. Shvo, *Organometallics* **1983**, *2*, 1689–1691.
[15] a) T. Mitsudo, Y. Hori, Y. Watanabe, *J. Org. Chem.* **1985**, *50*, 1566–1568; b) T. Mitsudo, Y. Hori, Y. Yamakawa, Y. Watanabe, *Tetrahedron Lett.* **1986**, *27*, 2125–2126; c) T. Mitsudo, Y. Hori, Y. Yamakawa, Y. Watanabe, *J. Org. Chem.* **1987**, *52*, 2230–2239.
[16] a) C. Ruppin, P. H. Dixneuf, *Tetrahedron Lett.* **1986**, *27*, 6323–6324; b) C. Ruppin, P. Dixneuf, *Tetrahedron Lett.* **1988**, *29*, 5365–5368; c) H. Doucet, J. Höfer, C. Bruneau, P. H. Dixneuf, *J. Chem. Soc., Chem. Commun.* **1993**, 850–851; d) H. Doucet, B. Martin-Vaca, C. Bruneau, P. H. Dixneuf, *J. Org. Chem.* **1995**, *60*, 7247–7255; e) H. Doucet, N. Derrien, Z. Kabouche, C. Bruneau, P. H. Dixneuf, *J. Organomet. Chem.* **1997**, *551*, 151–157.
[17] a) T. Opstal, F. Verpoort, *Tetrahedron Lett.* **2002**, *43*, 9259–9263; b) B. De Clercq, F. Verpoort, *J. Organomet. Chem.* **2003**, *672*, 11–16; c) K. Melis, D. De Vos, P. Jacobs, F. Verpoort, *J. Organomet. Chem.* **2003**, *671*, 131–136; d) K. Melis, F. Verpoort, *J. Mol. Catal. A* **2003**, *194*, 39–47.
[18] L. J. Goossen, J. Paetzold, D. Koley, *Chem. Commun.* **2003**, 706–707.
[19] M. Neveux, B. Seller, F. Hagerdon, C. Bruneau, P. H. Dixneuf, *J. Organomet. Chem.* **1993**, *451*, 133–138.
[20] a) K. Everaere, A. Mortreux, M. Bulliard, J. Brussee, A. van der Gen, G. Nowogroki, J.-F. Carpentier, *Eur. J. Org. Chem.* **2001**, 275–291; b) C. A. Sandoval, T. Ohkuma, K. Muñiz, R. Noyori, *J. Am. Chem. Soc.* **2003**, *125*, 13490–13503; c) P. Pelagatti, M. Carcelli, F. Calbiani, C. Cassi, L. Elviri, C. Pelizzi, U. Rizzotti, D. Rogolino, *Organometallics* **2005**, *24*, 5836–5844.
[21] D. Feichtinger, D. A. Plattner, *Chem. Eur. J.* **2001**, *7*, 591–599.
[22] D. Feichtinger, D. A. Plattner, P. Chen, *J. Am. Chem. Soc.* **1998**, *120*, 7125–7126.
[23] G. Gerdes, P. Chen, *Organometallics* **2004**, *23*, 3031–3036.
[24] a) P. Crochet, J. Gimeno, S. García-Granada, J. Borge, *Organometallics* **2001**, *20*, 4369–4377; b) P. Crochet, J. Gimeno, J. Borge, S. García-Granada, *New J. Chem.* **2003**, *27*, 414–420.
[25] S. M. O. Quintal, H. I. S. Nogueira, V. Félix, M. G. B. Drew, *J. Chem. Soc., Dalton Trans.* **2002**, 4479–4487.
[26] a) I. P. Evans, A. Spencer, G. Wilkinson, *J. Chem. Soc., Dalton Trans.* **1973**, 204; b) E. Alessio, G. Mestroni, G. Nardin, W. M. Attia, M. Calligaris, G. Sava, S. Zorzet, *Inorg. Chem.* **1988**, *27*, 4099–4106.
[27] P. E. Garrou, *Chem. Rev.* **1981**, *81*, 229–266.
[28] a) R. F. R. Jazzar, M. F. Mahon, M. K. Whittlesey, *Organometallics* **2001**, *20*, 3745–3751; b) T. Suárez, B. Fontal, M. Reyes, F. Bellandi, R. R. Contreras, E. Millán, P. Cancines, D. Paredes, *Transition Met. Chem.* **2003**, *28*, 217–219.
[29] V. Y. Kukushkin, *Coord. Chem. Rev.* **1995**, *139*, 375–407.
[30] a) J. C. Bryan, R. E. Stenkamp, T. H. Tulip, J. M. Mayer, *Inorg. Chem.* **1987**, *26*, 2283–2288; b) N. Koshino, J. H. Espenson, *Inorg. Chem.* **2003**, *42*, 5735–5742.
[31] a) A. M. Khenkin, R. Neumann, *J. Am. Chem. Soc.* **2002**, *124*, 4198–4199; b) F. J. Arnáiz, R. Aguado, M. R. Pedrosa, M. A. Maestro, *Polyhedron* **2004**, *23*, 537–543; c) K. Most, S. Köpke, F. Dall'Antonia, N. C. Mösch-Zanetti, *Chem. Commun.* **2004**, 1676–1677; d) A. Lehtonen, R. Sillanpää, *Polyhedron* **2005**, *24*, 257–265.
[32] J. P. McNamara, I. H. Hillier, T. S. Bhachu, C. D. Garner, *Dalton Trans.* **2005**, 3572–3579.
[33] J. S. Jaswal, S. J. Rettig, B. R. James, *Can. J. Chem.* **1990**, *68*, 1808–1817.
[34] J. Höfer, H. Doucet, C. Bruneau, P. H. Dixneuf, *Tetrahedron Lett.* **1991**, *32*, 7409–7410.
[35] P. S. Hallman, T. A. Stephenson, G. Wilkinson, *Inorg. Synth.* **1970**, *12*, 237–240.
[36] a) SAINT: SAX, Area Detector Integration, Siemens Analytical instruments INC., Madison, Wisconsin, USA; b) SADABS: Siemens Area Detector Absorption Correction Software, Sheldrick G., 1996, University of Goettingen, Germany; c) SMART for WNT/2000 version 5.622, Smart Software Reference Manual; Bruker Advanced X-ray Solution, Inc.: Madison, WI, **2001**.
[37] A. Altomare, M. C. Burla, M. Cavalli, G. Cascarano, C. Giacovazzo, A. Gagliardi, A. G. Moliterni, G. Polidori, R. Spagna, Sir97: A New Program For Solving And Refining Crystal Structures, **1997**, Istituto di Ricerca per lo Sviluppo di Metodologie Cristallografiche, CNR, Bari.
[38] G. Sheldrick, Shelxl97. Program for structure refinement. University of Göttingen, Germany, **1997**.
[39] L. J. Farrugia, *J. Appl. Crystallogr.* **1999**, *32*, 837.
[40] M. Nardelli, *J. Appl. Crystallogr.* **1995**, *28*, 659.
[41] a) F. H. Allen, O. Kennard, R. Taylor, *Acc. Chem. Res.* **1983**, *16*, 146; b) I. J. Bruno, J. C. Cole, P. R. Edgington, M. Kessler, C. F. Macrae, P. McCabe, J. Pearson, R. Taylor, *Acta Crystallogr., Sect. B* **2002**, *58*, 389.

Received: January 9, 2006
Published Online: April 20, 2006

